SYNTHESIS OF COBALT BASED METAL OXIDE NANOPARTICLES AND INVESTIGATION OF THEIR POTENTIAL USE AS CATALYSTS IN WATER OXIDATION REACTION

A THESIS SUBMITTED TO
THE GRADUATE SCHOOL OF NATURAL AND APPLIED SCIENCES
OF
MIDDLE EAST TECHNICAL UNIVERSITY

BY

İZEL AKSOY

IN PARTIAL FULFILLMENT OF THE REQUIREMENTS
FOR
THE DEGREE OF MASTER OF SCIENCE
IN
CHEMISTRY

MAY 2022

Approval of the thesis:

SYNTHESIS OF COBALT BASED METAL OXIDE NANOPARTICLES AND INVESTIGATION OF THEIR POTENTIAL USE AS CATALYSTS IN WATER OXIDATION REACTION

submitted by **İZEL AKSOY** in partial fulfillment of the requirements for the degree of **Master of Science** i**n Chemistry, Middle East Technical University** by,

Prof. Dr. Halil Kalıpçılar
Dean, Graduate School of **Natural and Applied Sciences** _____

Prof. Dr. Özdemir Doğan
Head of the Department, **Chemistry** _____

Prof. Dr. Emren Nalbant
Supervisor, **Chemistry, METU** _____

Examining Committee Members:

Prof. Dr. Gülsün Gökağaç Arslan
Chemistry, METU _____

Prof. Dr. Emren Nalbant
Chemistry, METU _____

Prof. Dr. Ayşen Yılmaz
Chemistry, METU _____

Prof. Dr. İrem Erel Göktepe
Chemistry, METU _____

Assoc. Prof. Dr. Oktay Demircan
Chemistry, Bogazici University _____

Date: 11.05.2022

I hereby declare that all information in this document has been obtained and presented in accordance with academic rules and ethical conduct. I also declare that, as required by these rules and conduct, I have fully cited and referenced all material and results that are not original to this work.

Name Last name: İzel Aksoy

Signature:

ABSTRACT

SYNTHESIS OF COBALT BASED METAL OXIDE NANOPARTICLES AND INVESTIGATION OF THEIR POTENTIAL USE AS CATALYSTS IN WATER OXIDATION REACTION

Aksoy, İzel
Master of Science, Chemistry
Supervisor: Prof. Dr. Emren Nalbant

May 2022, 53 pages

Fossil fuels have been accepted as a harmful energy source due to their destructive effects to the environment. Thus, extensive research have been conducted to find a renewable, clean and environmentally friendly energy sources. H_2 molecule is accepted as one of them because of its clean nature, light weight and high energy stored in its bond. It can be produced simply from the water splitting process using catalysts which are made from oxides of earth abundant metals. In this study, Co_2CrO_4 microspheres were hydrothermally synthesized as new electrocatalyst for water oxidation/oxygen evolution reaction (OER). SEM and TEM analyses revealed the hieararchical morphology of the microspheres which are assembly of nanoplates formed also by the assembly of individual nanoparticles with ca. 17 nm size. BET analyses showed that this new material has very high surface area (125 m^2 g^{-1}). Co_2CrO_4 microspheres were then used to modify glassy carbon electrode for electrocatalytic investigations in alkaline medium. The results revealed that this new material has promising catalytic performance towards OER with an onset potential of 1.52 V vs. RHE and an overpotential of 456 mV at 10 mA cm^{-2} current density. In addition, the microspheres presented very good stability during long-term constant potential electrolysis. In general, the catalytic performance of Co_2CrO_4 microshperes

are comparable to the one of benchmark RuO_2 with an advantage of being more stable and cost-effective.

Keywords: Clean energy, nanoparticles, spinels, water oxidation, electrocatalysts

ÖZ

KOBALT BAZLI METAL OKSİT NANOPARÇACIKLARIN SENTEZİ VE SUYUN YÜKSELTGENMESİ TEPKİMESİNDE KULLANILMAK ÜZERE KATALİZÖR OLARAK POTANSİYELLERİNİN ARAŞTIRILMASI

Aksoy, İzel
Yüksek Lisans, Kimya
Tez Yöneticisi: Prof. Dr. Emren Nalbant

Mayıs 2022, 53 sayfa

Fosil yakıtlar yıkıcı etkilerinden dolayı çevreye zararlı enerji kaynakları olarak kabul edilmişlerdir. Bu suretle; yenilenebilir, temiz ve çevre dostu enerji kaynakları bulabilmek için çokça araştırma yapılmaktadır. Temiz doğası, hafifliği ve bağlarında depolanabilen yüksek enerji sayesinde H_2 molekülü bu enerji kaynaklarından biri olarak kabul edilmektedir. Bu molekül, suyun ayrışması prosesi ile, doğada bulunan elementlerin oksitlerinden oluşan katalizörler yardımıyla kolayca üretilebilir. Bu çalışmada, Co_2CrO_4 mikroküreleri yeni bir katalizör olarak suyun yükseltgenmesi/oksijen çıkışı tepkimesinde kullanılmak üzere hidrotermal yöntemle sentezlenmiştir. SEM and TEM analizleri bu mikrokürelerin, boyutları 17 nm'yi bulan bireysel nanoparçacıklardan oluşan peletlerin birleşmesiyle oluşmuş bir morfolojiye sahip olduğunu göstermektedir. BET analizinin sonucunda mikrokürelerin oldukça yüksek yüzey alanına sahip olduğu ortaya çıkmıştır (125 m^2 g^{-1}). Camsı karbon elektrot yüzeyine yerleştirilen mikroküreler elektro-katalitik performans ölçümü için alkali ortamda test edilmiştir. Sonuçlar bu yeni materyalin 1.52 V vs. RHE başlangıç potansiyeli ve 10 mA cm^{-2} akım yoğunluğundaki 456 mV aşırı potansiyel ile ümit verici yeni bir katalizör olabileceğini göstermektedir. Ayrıca bu mikroküreler, uzun süreli sabit potansiyelli elektrolizde çok iyi kararlılık performansı göstermiştir. Genel olarak, Co_2CrO_4 mikroküreleri, kararlı ve ucuz

olması avantajlarıyla, RuO_2 gibi referans olarak kabul edilen diğer elektrokatalizörlerle kıyaslanabilecek özelliklere sahiptir.

Anahtar Kelimeler: Temiz enerji, nanoparçacıklar, spineller, suyun yükseltgenmesi, elektrokatalizörler.

To mother nature…

ACKNOWLEDGMENTS

I would first like to thank to Prof. Dr. Emren Nalbant for her open doors whenever I ran into a trouble spot or had a question about my research or writing. Without her great support, kindness, and friendly manner I could not complete this thesis. I am truly honored to have a chance to work with her.

I would like to thank Dr. Asude Çetin for her guidance during my laboratory work.

I would like to thank Prof. Dr. Ahmet M. Önal for his support during electrochemical measurements.

I would like thank Prof. Dr. Ayşen Yılmaz for access to the XRD instrument. Also, I would like to thank her group members for helping and teaching the techniques.

I would like to thank the Central Laboratory of METU for their help to take characterization measurements.

I would like to thank Scientific and Technological Research Council of Turkey (TUBITAK) for the financial support under Project No: 117Z384

I would like to express my thanks to Serra Kocabaş, Yağmur Ağcalı and all NanoClusMate Research Group members for their endless friendship and support.

Finally, I would like to thank my family, Ayşe and Hakkı Aksoy for being there for me with such a love and energy and make things easier for me. Also, I would like to thank my best friend Tutku Özcerit for her endless support and encouraging apple pies and my lovely partner Burak Ballı for his sweetness, patience and jokes which helps a lot during this process. I am truly lucky to have such a family.

TABLE OF CONTENTS

LIST OF TABLES

TABLES

LIST OF FIGURES

FIGURES

LIST OF ABBREVIATIONS

ABBREVIATIONS

BET	Brunauer – Emmett – Teller
Cdl	Double-layer Capacitance
CPC	Controlled Potential Coulometry
CTAB	Cetyltrimethylammonium Bromide
CV	Cyclic Voltammetry
DMF	Dimethylformamide
ECSA	Electrochemically Active Surface Area
EDX	Energy Dispersive X-Ray
FWHM	Full Width Half Maximum
GCE	Glassy Carbon Electrode
GSA	Geometric Surface Area
HER	Hydrogen Evolution Reaction
LSV	Linear Sweap Voltammetry
NTA	Nitrilotriacetic Acid
OER	Oxygen Evolution Reaction
RF	Roughness Factor
SEM	Scanning Electron Microscopy
TEM	Transmission Electron Microscopy
XPS	X-Ray Photoelectron Spectroscopy
XRD	X-Ray Diffraction

CHAPTER 1

INTRODUCTION

In recent years, the effects of climate change and resulted global warming have become more and more perceivable. Forest fires, floods and glacier melting etc. occur every day around the earth due to the climate change. There are lots of reasons which cause directly these outcomes such as deforestation and pollution. Especially, industrial pollution contributes these outcomes the most since it releases toxic materials to the environment.

Lots of solutions can be applied to eliminate the causes of the climate change. One of them is decreasing the usage of the fossil fuels. Burning fossil fuels to run the engines in daily or industrial life increases the amount of the greenhouse gases in the environment, thus, causes heat increase in the atmosphere. There are many researches which have been done in recent years to find an environmentally friendly alternative to the fossil fuels. Solar and wind power are widely used examples of energy producers. In addition to these examples, using H_2 gas as a fuel has been investigated since it is very promising and renewable energy source.

One of the ways to produce H_2 gas is water splitting which is an environmentally friendly, cost effective, simple and very successful method [1]. With the water splitting process H_2 gas is produced with electron transfers in simply two steps: hydrogen (HER) and oxygen evolution reaction (OER). These steps occur at cathode and anode, respectively[1–3]. The OER part of these steps requires transfer of four electrons to occur and this makes it kinetically more challenging than the HER and produces

large onset potential, an energy barrier, to achieve [4]. Using overpotential helps to decrease this energy barrier, but it also decreases the reaction rate and increases the energy that is needed for the reaction. The best way to overcome these drawbacks is catalyst usage for the OER part. The expectations for a good OER catalyst are given as high performance, good stability and economic availability and metal-oxides are very good candidates for these expectations [1]. Recently, researchers have interested in the noble metal-oxide nanoparticles as catalysts such as IrO_2 and RuO_2 since they show remarkable performances with OER. Lee et al. found that the onset potential of rutile RuO_2 as 1.48 V vs RHE, but they also state that this remarkable catalytic performance can be detected only in acidic medium [5]. Similarly, Yang et al. state that RuO_2 has a very astonishing catalytic ability with an onset potential of 1.47 V (vs RHE) and 255 mV overpotential at η_{10} [6]. Suen et al. also state that RuO_2 and IrO_2 are very good OER catalyst candidates, but they are unstable as they go to higher oxidation states [3]. The disadvantages such as high cost and low stability in alkaline medium, these catalysts have directed the researchers to find more suitable catalysts, especially industrial scale processes. Therefore, catalysts synthesized from earth-abundant elements' oxides (i.e., Co, Cr, Fe, Mn, Ni, etc.) draw the attention the most and stands as alternatives to eliminate these disadvantages since they show good stability and economically friendly properties.

These earth-abundant metals can be used as catalysts in different forms. While single-metallic ones show very good catalytic activity, multimetallic ones provide other elements' properties to the catalytic process. Different combinations of different earth-abundant elements give unique results as catalysts. As an example, the electrocatalytic activity of $NiFe_2O_4$/NF have been investigated by Fang et al. for OER process, and they found that the overpotential of $NiFe_2O_4$/NF was 293 mV at the current density of 10 mA cm^{-2}, which is comparable to the ones reported with RuO_2[7]. Another example of combination of earth-abundant elements' oxides, $MnCo_2O_4$, is reported by Sun et al. and they found that $MnCo_2O_4$@NC is an outstanding electrocatalyst for water oxidation reaction demonstrating 287 mV

overpotential to overcome a current density of 10 $mA \cdot cm^{-1}$ [8]. Li et al. reported a research on spinel ferrites, MFe_2O_4 (M = Co, Ni, Cu, etc.), and their catalytic performance on OER, found that cobalt integrated ferrite spinel particles have better performance in OER than the others[9]. Liu et al. work on $NiO/NiFe_2O$ nanorods as OER catalyst and found that its overpotential at 10 mA cm^{-2} is 302 mV with a Tafel slope of 42 mV dec^{-1} [10]. Another study was conducted by Zhao et al. for the investigation catalytic properties of urchin like $NiCo_2O_4$ spheres and it is reported that the combination of nickel and cobalt as catalyst has unique cycling stability in cyclic voltammetry [11].

Numerous study report that arrangement of the transition metals such as nickel, cobalt, chromium and iron as spinel structures provides remarkable catalytic performance in OER/HER. Especially, the cobalt based ones have been widely investigated. Wei et al. reported that $NiCo_2O_4$ nanowires which are highly oxygen deficit can be used for HER since they exhibit a low overpotential, 104 mV to reach 10 mA cm^{-2} and they are very durable at 100 mA cm^{-2} [12]. Ekebas et al. investigated magnesium substituted cobalt nanostructures for water oxidation reaction and reported that urea-stabilized $MgCo_2O_4$ (U-$MgCo_2O_4$) and NTA- stabilized ones (NTA-$MgCo_2O_4$) have require lower overpotentials, 463 mV and 573 mV to get 10 mA cm^{-2} current density [13]. Cetin et al. also reported that $NiCo_2O_4$–NiO nanoparticles which are synthesized with different surfactants (Urea and CTAC). These particles have very good catalytic performances with onset potentials of 1.56 V vs RHE for U–NiCo and 1.57 V vs RHE for C–NiCo, U–NiCo and overpotential values of 387 mV and 430 mV, respectively [14]. In their article about investigating the effect of reducing Jahn-Teller distortion in cobalt-based electrocatalysts which causes poor activity and stability, Ge et al. found that $MnCo_2O_4$@NiP_2 a very promising OER electrocatalyst with a very good activity with a tafel slope of 113 mV dec^{-1} and an overpotential of 240 mV at 10 mA cm^{-2} in alkaline medium [15]. Shan et al. reported a research on the catalytic performance of iridium integrated cobalt spinel oxide particles as OER catalysts and found that their catalyst have at least 2

orders of magnitude higher activity in acidic medium than cobalt oxide itself because of the strong interactions between cobalt and iridium elements [16]. In the research of Selvakumar et al., silica-derived spinel cobalt oxide particles have been investigated for their catalytic activity in OER and the found that among the examples that they investigate, MCM-48 derived Co_3O_4 gives remarkable OER performance with an observed potential of 1.76 V at 10 mA/cm^2 and a Tafel slope of 107 mV dec^{-1} [17]. As a last example, Hong et al. investigated the catalytic activity of nickel-doped Mn_3O_4 nanoparticles as catalysts for water oxidation process and reported that nickel integration provides lattice distortion, thus, it strongly enhances the OER activity which resulted as an overpotential of 458 mV at η_{10} under neutral conditions [18].

With the aspect of the examples, different metal integrated cobalt-based spinel-type nanomaterials in various morphologies drew the attention because of their remarkable OER activity. Maiyalagan et al. reported that at 10 mA cm^{-2} current density, the $Ni_{1.5}Co_{0.75}Mn_{0.75}O_4$ catalyst overpotential is 1.80 V for OER, which is a multimetallic example of the catalysts [19]. Cheng et al. investigated $ZnCo_2O_4$/CNTs' catalytic performance and show it has a good OER activity and an onset potential of 1.65 V [20]. Zhu et al. reported that the combination of Ni–Co_2–O shows astonishing catalytic activity in OER with the onset potential of 1.501 V and a small overpotential of 0.362 V at the current density of 10 mA cm^{-2} [21]. Another example of cobalt-based spinel catalyst came from Gardner et al. reporting that $LiCoO_2$ nanoparticles for OER catalysis have overpotential of ~420 mV at 10 mA cm^{-2} at alkaline medium[22]. Also, Khan et al. reported a research on silica-based mesoporous core shell cobalt oxides (Co_3O_4@SiO_2) showing relatively low overpotential value, 529 mV at a current density of 10 mA cm^{-2} [23]. All of these examples show that the synergetic effect between the metals such as Fe, Ni, etc. with Co and even oxide of Co itself show remarkable catalytic performance which is considerably better than the constituent elements' oxides.

Numerous metal-incorporated cobalt oxides mentioned above (i.e., Co_3O_4, $LiCo_2O_4$, $NiCo_2O_4$, $CuCo_2O_4$, $MgCo_2O_4$, $FeCo_2O_4$, $ZnCo_2O_4$ and $MnCo_2O_4$) have been evaluated for their catalytic performances in OER. Among all the cobalt-based spinel oxides, chromium integrated cobalt oxide has been considered as a preferable material for lots of applications. As an example, Yazdanbakhsh et al. used Co_2CrO_4 nanomaterials for oxidation of sulfides to sulfoxides [24]. Another example of usage of chromium integrated cobalt oxide nanoparticles came from Zhao et al. reporting yolk–shell structured Co_2CrO_4 nanospheres as catalysts for batteries[25]. Similarly, Lin et al. investigated the catalytic performance of Co_2CrO_4 nanopowders for proton-conducting fuel cell reactors[26]. Also, Ge et al. reported usage of $Co_2CrO_4/Co_1{-}xS$ as high-performance supercapacitor[27]. In spite of these various research areas of chromium integrated cobalt oxide particles, there have been no reports up until now on these nanomaterials in Co_2CrO_4 spinel structure as catalyst for water splitting process to our knowledge.

In the view of these information, in this thesis study; the synthesis, characterization, and investigation of OER performance of chromium integrated cobalt oxide materials have been investigated as water oxidation catalysts. The simple hydrothermal method was used for the synthesis of the material. The synthesis yielded microspheres, which are formed by the assembly of nanoplates. The microscopy investigation reveals that nanoplates are assembled by Co_2CrO_4 nanoparticles and has hierarchical structure. The electrocatalytic measurements result that the Co_2CrO_4 microspheres shows enhanced catalytic performance in alkaline medium and the catalytic performance is comparable or higher than that of the results of another metal oxide compositions in the literature.

1.1 Climate Change, Reasons and Methods to Prevent It

Climate change or global warming is the fact that the long term rises in temperature of the planet Earth. This situation is caused by the increasing greenhouse effect and harmful gases released to the atmosphere caused by mainly the human actions such as excessive usage of fossil fuels, deforestation and wrong farming.

As mentioned above the source of climate change is the greenhouse gases, and the increased carbon dioxide level in the atmosphere causes that greenhouse effect. Burning fossil fuels to generate electricity or using them as fuels in vehicles releases excessive amount of carbon dioxide to the atmosphere and, since carbon dioxide plays very important role in climate change, it should be decreased to optimum levels. Plants and trees absorb carbon dioxide to produce oxygen gas by photosynthesis. Oxygen gas is very essential for the living organisms. But, the actions such as deforestation kills the livings which produces that very important molecule for the continuation of the life. As a result of deforestation, the carbon dioxide which is released to the atmosphere cannot be consumed and high levels of carbon dioxide causes greenhouse effect. Also, wrong farming is another cause of the climate change. Increasing demands and overconsumption of the societies causes destruction in nature. Actions such as farming using pesticides, excessive amount of meat consumption and hunting changes the balance in the nature, thus, are destructive. These situations result increasing temperature among the planet and the changes in the harmony of the nature results with the climate change.

Despite to the reasons and the actions that cause climate change, the long-term outcomes of global warming can be prevented by simply decreasing the release of greenhouse gases. In addition to the simple solutions in daily life, strict regulations can and should be applied to decrease the overconsumption such as banning illegal

farming or hunting and preventing deforestation. All of these solutions decrease the carbon dioxide release and consequently prevent the climate change.

1.2 Water Splitting

Among all of the solutions mentioned before, one of them is much more effective to decrease carbon dioxide release: clean energy usage. Using clean energy as fuel instead of burning fossil fuels provides fundamental decrease in greenhouse effects since they do not contain carbon materials.

Clean energy sources can be various types such as wind power, solar power, biomass and hydrogen gas as a fuel. Among them hydrogen gas as a clean and renewable energy source draws significant amount of interest because of its working principle: water splitting. Simply the water is splitted to hydrogen and oxygen gas; while hydrogen gas is used as fuel, oxygen gas is released. For the combustion of hydrogen gas, the oxygen in the air is used and the product again will be the water. This cycle goes on and provides renewable energy for our planet.

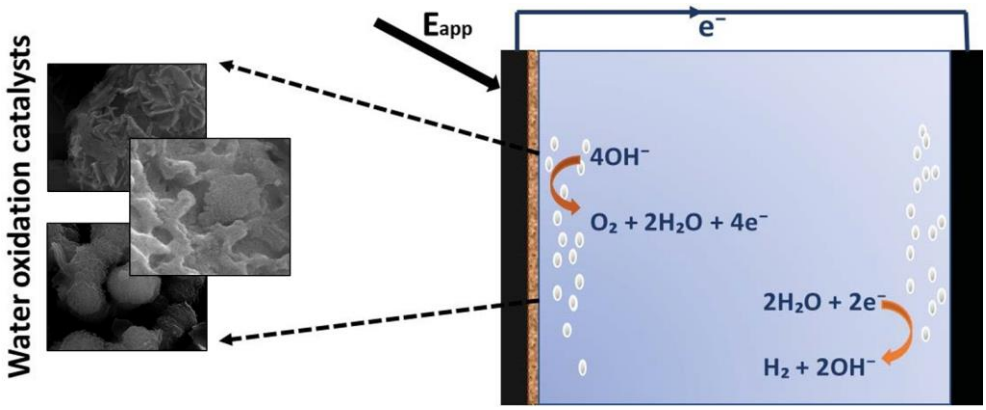

Figure 1.1 Schematic representation of electrochemical water splitting process[1].

The water splitting or the water oxidation process is an environmentally friendly and very promising method to produce hydrogen gas. In this work, electrochemical water oxidation process was used:

Oxidation half-reaction: $2H_2O \rightarrow O_2 + 4H^+ + 4e^-$ (OER)

Reduction half-reaction: $2H^+ + 2e^- \rightarrow H_2$ (HER)

Overall water splitting reaction: $2H_2O \rightarrow O_2 + 2H_2$

Simply, the overall process includes hydrogen (HER) and oxygen evolution reaction (OER). It requires both thermodynamically and kinetically high energy. Especially, the OER is kinetically more challenging than HER since it requires transfer of four electrons and thus large onset potential [1,4]. Therefore, electrocatalyst usage is necessary to get high performance and stability.

In recent years, lots of researches were performed about the water oxidation catalysts. Especially, usage of metals to synthesize catalysts and their electrocatalytic activity has been investigated for the oxygen evolution reaction. Among all of the researches, catalysts which were synthesized using Iridium and Ruthenium metals draw a significant attention. The oxides of these noble metals (IrO_2 and RuO_2) have been proved as the best catalysts as they show the highest catalytic activity for OER since the reactions with them give onset potentials approximately 1.4 V vs. RHE which is the closest value to the one with oxidation half reaction of water (1.23 V vs. RHE) [5,6].

Although researches prove that they have the highest catalytic activity in both acidic and alkali medium, these catalysts have drawbacks to prevent them to be used in long term usage. One of the reasons is that they are very expensive since they are rarely abundant on Earth. Also, they are unstable in high oxidation states. That is why, scientists investigate other potential catalysts to perform water splitting process.

Metal oxide particles are the particles which consist of a metal cation and an oxide anion. The formation of these particles occurs due to the electron transfer which take place in between the metal and oxygen atoms. These crystalline formed particles have unique physical and chemical properties; thus, they have been used in various applications up to now. The reason behind this popularity of metal oxides is that their properties can be arranged simply by changing the metal in the particles. These simple changes provide different electron orientation, different oxygen vacancies and consequently structural difference. As a result, their properties can be arranged according to the area of interest.

In the case of water splitting process, the usage of the metal oxides, especially the ones formed with transition metals, have been widely investigated. Since using these metals improve the catalytic performance resulted from very active electron transfer properties, they are used as electrocatalysts in electrochemical measurements. The following reactions proposes a mechanism indicating how transition metal catalysts performs the oxygen evolution reaction in water splitting process.

$$M + OH^- \rightarrow M - OH + e^-$$

$$M - OH + OH^- \rightarrow M - O^* + H_2O + e^-$$

$$M - O^* + OH^- \rightarrow M - OOH + e^-$$

$$M - OOH + OH^- \rightarrow M - O_2 + e^-$$

$$M - O_2 \rightarrow M + O_2$$

Figure 1.2 Proposed reaction mechanism of transition metal oxides in water splitting process[1]. M represents the active site on the catalyst.

1.3 Transition Metal Oxide Particles

In this work, the working principles of transition metal oxides are used for the catalytic process. Transition metals are the metals which are placed generally in between the third and twelfth rows of the periodic table. These metals have partially filled d-orbitals which provide very effective power on accepting and donating electrons. By the help of this property, they can easily change their oxidation states which will be very helpful in electron transfer processes [28,29]. This work is especially interested in the elements Cobalt and Chromium which are placed in the first row of

the transition metals. Since these first-row transition metals provide higher abundance and feasibility than the ones in the other rows, they are economically preferable and prone to give better results in many areas of researches [30].

In recent years, multimetallic oxides, especially in spinel structures have been investigated widely for their catalytic usage for OER/HER and among all these researches, transition metal oxides draw the attention the most for their catalytic performance. Transition metal oxides can form crystalline structures in various forms such as monoxides, dioxides, perovskites and spinels. Spinel structures are generally represented as AB_2O_4 (Figure 1.2), where A and B are metal cations. The A cations fill the one-eighth of the tetrahedral holes while B cations fill half of the octahedral holes, and with this configuration the whole structure shows ccp array. Charge neutrality in spinel structures arranged with either +2 and +3 ($A^{2+}B_2^{3+}O_4^{2-}$) or +4 and +2 ($A^{4+}B_2^{2+}O_4^{2-}$) oxidation states and according to the cation distribution between the tetrahedral and octahedral holes they become normal, inverse or complex spinel structures[1].

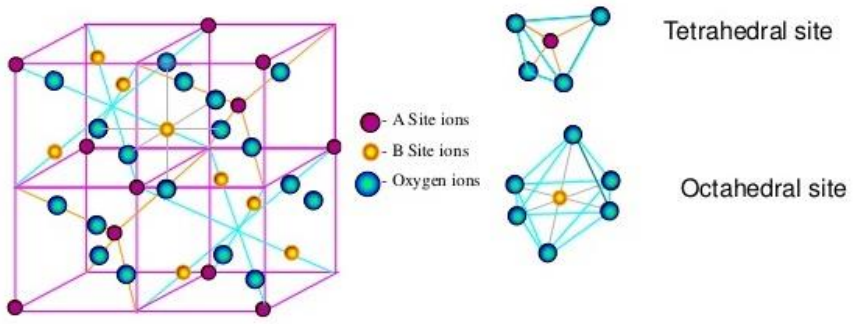

Figure 1.3 Schematic representation of spinel structure[2].

In this work, the catalyst that has been used has inverse spinel form. In the inverse spinel case, all of the metal A and half of the metal B hold the octahedral sites and

the other half of the metal B occupy the tetrahedral sites. The difference between spinel and inverse spines structures are caused by the crystal field stabilization energy[1,31].

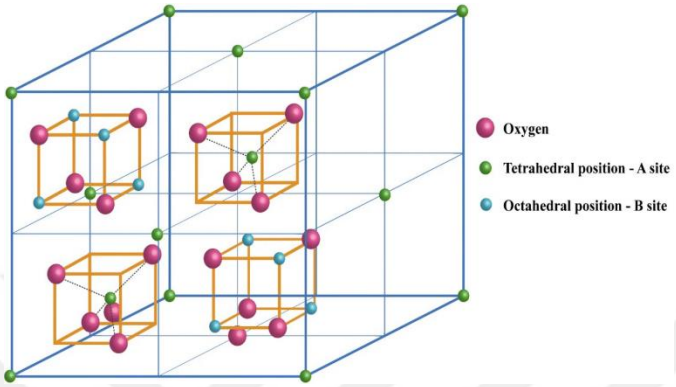

Figure 1.4 Inverse spinel structure [32].

1.4 Synthesis of Transition Metal Oxide Nanoparticles

Transition metal oxide particles can be synthesized in various ways. Different synthesis methods result in different structured and shaped particles. In general, the synthesis approaches of nanoparticles are divided into two main categories: bottom-up and top-down approaches. Top-down approach is a simple physical synthesis method which is mainly crushing of materials into dust by grinding. However, there are some drawbacks of this process even though the simplicity of it makes it desirable for the synthesis process. With top-down approach there is no control over size and shape of the particles[33]. Therefore, more useful technique, bottom-up approach is more preferable for the synthesis of nanoparticles. With the help of bottom-up synthesis the desired shape and size of the particles can be achieved. Additionally, this method has variety of techniques which involves physical and chemical

processes such as vapor-phase, solution-phase and solid-phase reactions. In this work, solution-phase bottom-up approach has been taken as synthesis method using sol-gel and hydrothermal processes.

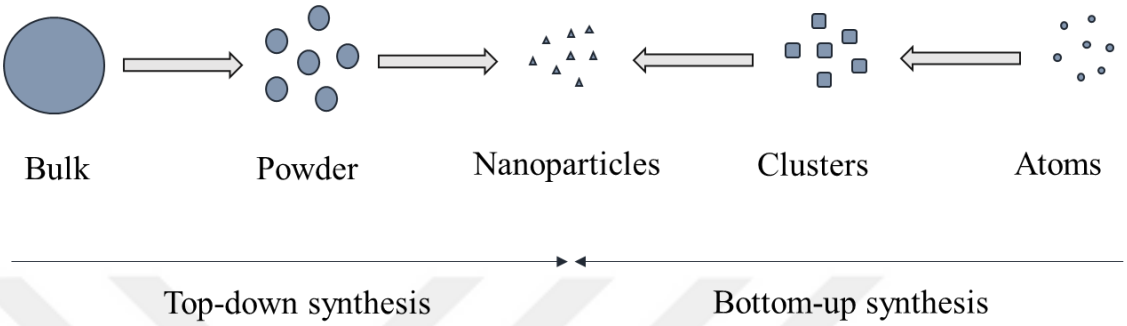

Figure 1.5 Schematic representation of bottom-up and top-down synthesis methods.

1.4.1 Sol-Gel Process

This simple polymerization process is one of the techniques that is widely used for nanoparticle synthesis. The name ‘sol-gel’ comes from the main steps of the process. ‘Sol’ step is the very first step of the process which the preparation of the solution is done with the necessary ingredients. After this step, the second step ‘gel’ formation occurs which indicates the formation of an inorganic interconnected polymeric material. The third step of the sol-gel process is aging of the gel to solidify the product. After these; the finishing steps, simply drying and dehydration with thermal treatment are applied to get the desired product [33–36]. Different choices of the surfactants, precursors, heat etc. which are applied during the process will provide control over shape and size of products.

1.4.2 Hydrothermal Process

Hydrothermal method is also one of the most preferrable methods like sol-gel method since it provides cheapness and ease to practice. This method also provides control over size, shape and morphology of the nanoparticles produced[1,35]. It requires solvents, surfactants, and precursors at the beginning. As the name indicates, the solvent used for this process is water (sometimes the water is supported with other solvents such as alcohol derivatives). The other ingredient is the surfactant which provides stabilization in between the surfaces of the reactants and directs the size and the shape of the particles. Lastly, a suitsble precursor is used to supply the main components (such as the metals) to the medium[8]. The combination of these solvents, surfactants and precursors can be adjust to reach the intended product with intended qualities. After mixing the ingredients the reaction goes on in a Teflon vessel inside of an autoclave, as a result, high temperature and pressure is reached. In this process, with the help of this adjustable high temperature and pressure, very small particles with desired morphologies can be produced.

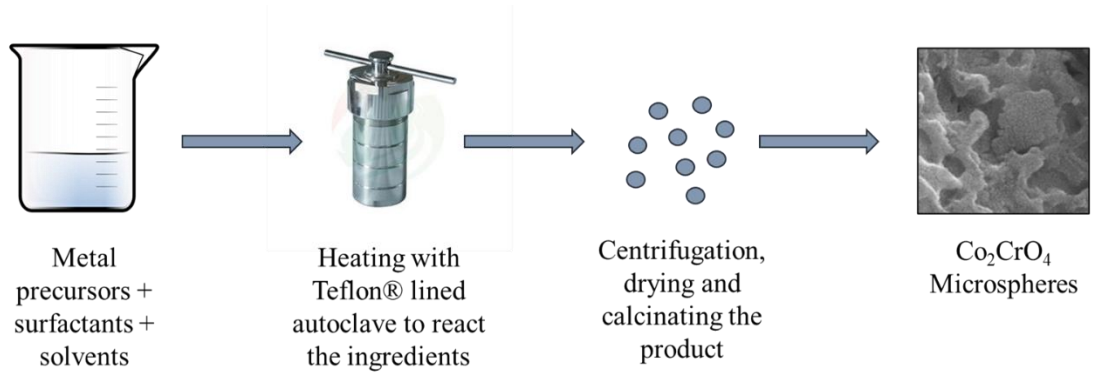

Figure 1.6 Schematic representation of Hydrothermal Process

1.5 Characterization of Transition Metal Oxide Nanoparticles

The synthesized nanoparticles are then analytically characterized to know whether they have provided desired properties or not. These characterization reveals the structure, morphology and composition of the nanoparticles. Commonly used characterization techniques are; electron microscopies which are Scanning Electron Microscopy (SEM) and Transmission Electron Microscopy (TEM), Energy Dispersive X-Ray Spectroscopy (EDX), X-Ray diffraction (XRD) analysis and X-Ray photoelectron spectroscopy (XPS).

Electron microscopes are used to investigate the surface topography, morphology, size and shape of the nanoparticles. In particular, **SEM** helps to understand the surface topography. Unfortunately, it provides poor resolution in atomic scale. With the help of another electron microscope, **TEM**, more detailed information about nanoparticles' size, shape and composition can be provided. The information provided by SEM and TEM can be supported by **EDX** analysis to get the basic elemental distribution.

The crystal structure and the chemical composition of the synthesized nanoparticles can be determined by **XRD analysis**. While the X-Ray patterns help to understand the identification of the material using characteristic peak sets, the size of the crystallites can be determined by Debye-Scherrer equation with the help of X-Ray [37].

$$\tau = \frac{\kappa\lambda}{\beta cos\theta} \qquad (1.1)$$

In the equation 1.1, while τ indicates crystallite size, κ and λ indicates dimensionless shape factor, and wavelength (nm) of X-Ray. Line broadening (radian) at full width half maximum (FWHM) and the Bragg angle are indicated with β and θ.

X-Ray Photoelectron Spectroscopy (XPS) is both a quantitative and qualitative technique for nanoparticle characterization. The surface characterization of the synthesized nanoparticles is analyzed by XPS. While with the help of the photoelectrons emitted from the surface at certain energy levels helps to determine the chemical and electronic state of the constituent elements, the concentrations and the surface distribution of these elements can also be detected by XPS.

Brunauer-Emmett- Teller (BET) isotherm is a common analysis method which is used to determine the surface area, pore size and volume of the synthesized material. It also helps to identify the porosity of the material via adsorption-desorption mechanism.

1.6 Important Parameters for Water Oxidation Catalyst Activity

To understand the performance of water splitting catalyst, several parameters should be considered such as overpotential, Tafel slope, onset potential, capacitance and stability. The techniques such as cyclic voltammetry (CV), linear sweep voltammetry (LSV), controlled potential coulometry and chronoamperometry etc. which help to state these electrochemical parameters for a catalyst.

Linear Sweep Voltammetry (LSV) is one of the very important tools to evaluate these parameters. With the help of LSV polarization curves of the catalysts are

obtained. Parameters such as onset potential, overpotential and Tafel slope are reported from these curves. The point where the water oxidation process starts is accepted as onset potential and this point generally meets with the potential of 10 μA cm^{-2} current density [1]. Intersecting tangent lines from one at the faradaic region where the current density increase is observed while other at the non-faradaic region also gives the **onset potential** value [1]. The expectation from a good catalyst is to have a low onset potential (close to water itself) meaning higher catalytic activity [38].

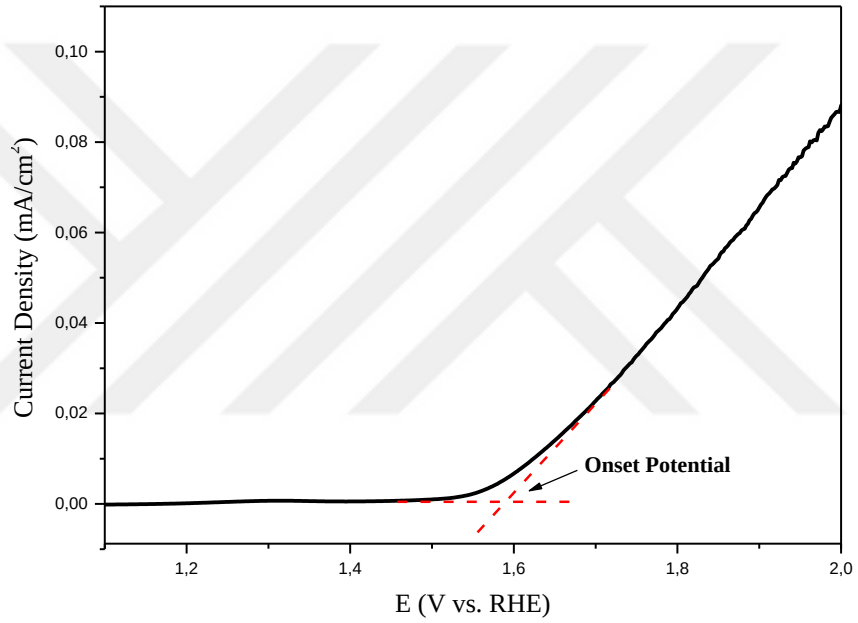

Figure 1.7 Onset potential determination from polarization curve.

The potential difference between the applied potential and the equilibrium potential is called the **overpotential**. Although it is expected that the difference between these potentials is zero, to conduct the reaction and achieve the kinetic barrier of the reaction higher applied potential than equilibrium potential can be used (REF). Even so, a low applied potential, thus, a low overpotential is expected from a good water

splitting catalyst[1]. A simple equation can be used to calculate the overpotential value, η:

$$\eta = E - E_{eq} \quad (1.2)$$

Where E and E_{eq} represents the applied and the equilibrium potential respectively.

When a catalyst is mentioned, the reaction rate is very important. **Tafel slope** provides data about the rate determining step and the reaction mechanisms. It can be determined by linear fitting of the polarization curves [35].

$$\eta = a + b.\log(j_o) \quad (1.3)$$

While η, a and j_o indicate the overpotential, the intercept and exchanged current density respectively and b represents the Tafel slope. Lower Tafel slope is expected to get a faster reaction.

Electrochemical measurements are done by catalyst loading on an electrode surface. This loading creates a double-layer between electrolyte and the catalyst which occurs due to charge collection and provides capacitance like behaviour of the electrode. **Double-layer capacitance (Cdl)** is important since it helps to understand how many atoms are involved the catalysis process. It is helpful to use cyclic voltammetry measurements in a non-faradaic potential range (v) at various scan rates to determine the value of the double-layer capacitance (Cdl); which the measured current is accepted as the double-layer charging current (idl). The slope of the idl versus non-faradaic potential (v) plot gives the Cdl value[1].

The capacitance of this double-layer and the **electrochemically active surface area (ECSA)** of the catalyst loaded electrode are directly proportional to each other and provides information about how many of the atoms in the catayst have the catalytic performance and participate the catalysis process. ECSA can be calculated using the following formula:

$$ECSA = Cdl / Cs \quad (1.4)$$

which Cs indicates specific capacitance of the material.

Roughness Factor (RF) is another parameter that defines the catalytic performance of the material and it can be calculated as:

$$RF = ECSA / GSA \quad (1.5)$$

where GSA represents the geometric surface area of the electrode. The expectation from a good catalyst is to give higher values of Cdl, ECSA and RF since they represent larger active sites and consequent better catalytic activity.

Stability is another factor to determine the catalytic performance of an electrocatalyst. Stability measurements can be conducted applying electrolysis at constant potential to the modified electrode for a time and the fluctuations in the current density is tracked. These measurements are also supported with the polarization curves which are taken at the beginning and the end of the constant potential electrolysis. The expectation from a stable catalyst is to show no change or

at most a minor change in the current density and the other electrochemical parameters.

1.7 Motivation of This Study

The energy sources that are used today are consumed day by day and creates climate change. The need of renewable and clean energy sources for the future creates new research areas. One of these clean energy sources is hydrogen gas. Because of its energy carrying and storage ability, it draws attention in several industries. This small molecule can easily be separated from water using water oxidation reaction. But, kinetically and thermodynamically, the water oxidation process is not easy and suitable catalysts are needed.

For a long time, RuO_2 and IrO_2 are known as the best water oxidation catalyst because of their low overpotentials and onset potential values (e.g. 1.48 V vs. RHE onset potential for RuO_2). Unfortunately, these elements which form the catalysts are rare and very expensive and the catalysts are not stable in alkaline mediums for long times. Hence, it is needed to design a new and more effective catalyst from earth abundant metals with desired catalytic performances.

In recent years, nanomaterials which are oxides of earth-abundant elements are widely investigated in water splitting researches. Especially, transition metal oxides with various metal combinations give remarkable results as electrocatalysts in water oxidation process. Therefore, in this thesis study a new and promising catalyst, Co_2CrO_4 microspheres, is investigated for its catalytic performances. To show its properties, the aim for this work is to conduct the following studies:

- Synthesis of Co_2CrO_4 microspheres via hydrothermal method.
- Characterization of Co_2CrO_4 microspheres by various analytical techniques that are XRD, EDX, SEM, TEM, XPS and BET.
- Investigation of the electrocatalytic performance of Co_2CrO_4 microspheres as water oxidation catalyst.

CHAPTER 2

EXPERIMENTAL

2.1 Materials

All reagents were utilized as purchased. No further purifications were needed. Cobalt (II) nitrate hexahydrate ($Co(NO_3)_2 \cdot 6H_2O$), chromium nitrate nonahydrate ($Cr(NO_3)_3 \cdot 9H_2O$), hexadecyltrimethylammonium bromide (CTAB), isopropyl alcohol, and Nafion® solution (5% wt.) were obtained from Sigma-Aldrich. Aqueous solutions were prepared using deionized ultrapure water (resistivity>18 MΩ, PURELAB Option-Q, ELGA).

2.2 Synthesis of CTAB-Co_2CrO_4 Microspheres via Hydrothermal Method

Simple and common hydrothermal method was chosen to synthesize CTAB-stabilized Co_2CrO_4 nanostructures[8]. 6.0 mmol of cobalt (II) nitrate hexahydrate ($Co(NO_3)_2 \cdot 6H_2O$), 3.0 mmol of chromium nitrate nonahydrate ($Cr(NO_3)_3 \cdot 9H_2O$) and 4.7 mmol of CTAB were added to deionized water (10.0 mL) and isopropyl alcohol (30.0 mL) mixture and stirred until complete dissolution of the reactants. The obtained dark blue solution was transferred into a Teflon-lined stainless-steel autoclave and heated to 180 °C for 6 h. After that, the obtained precipitate was separated from solution by centrifugation and washed with deionized water and ethanol. Finally, the precipitate was dried at 60 °C for 8 h and calcined at 350 °C for 1 h. After calcination process, black powder of Co_2CrO_4 microspheres is collected.

2.3 Materials Characterization

The transmission electron microscopy (TEM) measurements were carried out on FEI Tecnai G2 F30 electron microscope operating at 300 kV. FEI Nova Nano SEM 430 was used to get scanning electron microscopy (SEM) images of Co_2CrO_4 microspheres. The elemental composition of the materials was analyzed with energy-dispersive X-Ray (EDX). X-ray diffraction (XRD) analyses were done on Rigaku Ultima IV X-ray diffractometer with Cu Kα radiation (λ = 1.54 Å) in the 2θ range from 10° to 80°. X-ray photoelectron spectroscopy (XPS) analyses was performed with PHI-5000 VersaProbe (Physical Electronics (PHI) Chanhassen, Minneapolis, MN) which has Al Kα (1486.92 eV) source. The XPS data were calibrated to C1s peak at 282.0 eV. Brunauer-Emmett-Teller (BET) analysis with Autosorb-6 (Quantachrome Corporation) instrument was performed to assess pore volume and surface area of the microspheres. Dehydration of samples was carried out at 300 °C for 5 h before the analysis.

2.4 Electrochemical Characterization

2.4.1 Electrode Preparation

Electrochemical measurements are carried out with glassy carbon electrodes (GCE) to investigate the characteristics of Co_2CrO_4 microspheres. GCEs has 0.07 cm^2 surface area and they were modified as working electrodes and used accordingly in the experiments.

Electrodes are prepared with the help of the method reported by Kuo et al. [39]. 11.2 mg catalysts and 2.0 mL dimethyl formamide (DMF) were mixed together vigorously, and the solution was sonicated for 30 minutes. Then, 19 µL Nafion® solution was added to the mixture. After 2 more hours additional sonication, 5.0 µL of the homogeneous solution was planted onto the GCE surface and left to dry in an oven at 90 ºC for 24 h. The catalyst loading by mass for 0.07 cm² surface of the electrode was determined as 0.4 mg. For comparison, RuO_2 and Co_3O_4 was also characterized following a previously reported procedure and used as benchmark the Co_2CrO_4 catalyst [40,41].

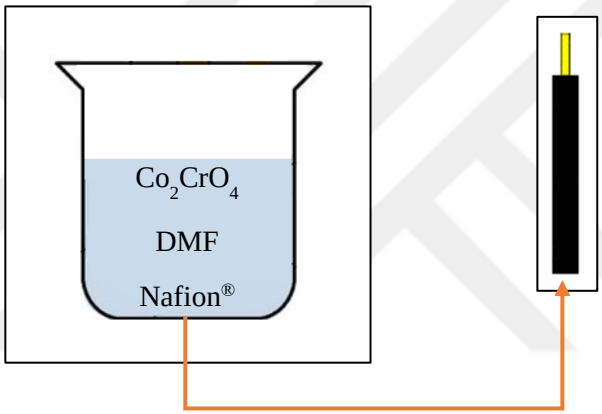

Figure 2.1 Preperation of glassy-carbon electrode with DMF and Nafion®

2.4.2 Electrochemical Measurement

Electrochemical characterization was carried out with Gamry 1010B potentiostat-galvanostat. The measurements were performed in a standard three-electrode system in alkaline medium of 0.1 M KOH at room temperature. The system is constructed with Ag/AgCl (in 3.0 M NaCl) and Pt wire as reference and counter electrodes, respectively. Polarization curves were recorded to evaluate the electrochemical

properties. The potentials (vs. Ag/AgCl) were reported against reversible hydrogen electrode (RHE) and this was determined by Nernst equation[1]:

$$E_{RHE} = E_{Ag/AgCl} + 0.059\ pH + E^{\circ}_{Ag/AgCl} \qquad (E^{\circ}_{Ag/AgCl} = 0{:}198\ V) \qquad (2.1)$$

The overpotential values were calculated by the following equation:

$$\eta = E_{RHE} - 1.23\ V \qquad (2.2)$$

As mentioned before, linear fitting of the polarization curves gotten from previous measurements to Tafel equation provides the reaction kinetics of Co_2CrO_4 microspheres in water splitting process (Equation 1.3).

The modified electrode was then evaluated by controlled potential electrolysis in alkaline medium (0.1 M KOH) to understand the stability of the catalyst. The electrochemically active surface area (ECSA) of the catalyst is very important to understand the catalytic performance. The double-layer capacitance (Cdl) values were taken by cyclic voltammograms (CVs) measured at non-Faradaic region of 0.0-0.1 V (vs RHE) at scan rates of 5-10-15-20 mV s^{-1} to evaluate the ECSA. The slope of double-layer charging current at 0.1 V (vs RHE) versus scan rate gives the Cdl values for the catalyst. Then, the ECSA values were calculated using the equation 1.4. The surface roughness factor (RF) was determined simply by dividing ECSA of the catalyst to the electrode geometric surface area (GSA) (Equation 1.5).

Another important parameter, the mass activity (A g^{-1}) was calculated using the following equation at a certain overpotential[42]:

Mass activity = j / m (2.3)

In the equation, m (mg cm^{-2}) and j (mA cm^{-2}) imply the catalyst loading and the current density, respectively.

Finally, the specific activity of the catalyst was calculated using the following equation [43]:

Specific activity = i / ECSA (2.4)

where i is the current at a specific potential.

CHAPTER 3

RESULTS AND DISCUSSION

3.1 Characterization of Surface and Structural Properties of Co_2CrO_4 Nanoparticles

Synthesis of CTAB-Co_2CrO_4 microspheres were done by applying a simple hydrothermal method where CTAB was used as a structure-directing agent (Figure 3.1). SEM and TEM images of Co_2CrO_4 nanostructures at different magnifications were demonstrated in Figure 3.2. With the help of the SEM images, it can be understood that the synthesis of the catalyst via the hydrothermal method with CTAB resulted the formation of microspheres which is sized as 1.25 µm ± 0.15 µm and these microspheres are assembled by nanoplates with nonuniform morphologies. At higher magnifications in SEM, the images show that the nanoplates are also assembly of individual NPs (Figure 3.2 (a-c)).

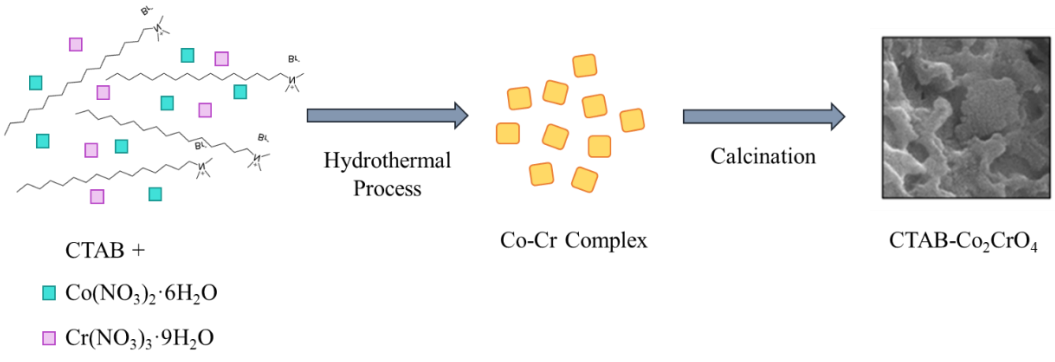

Figure 3.1 Illustrative representation of formation of CTAB-Co_2CrO_4 microspheres.

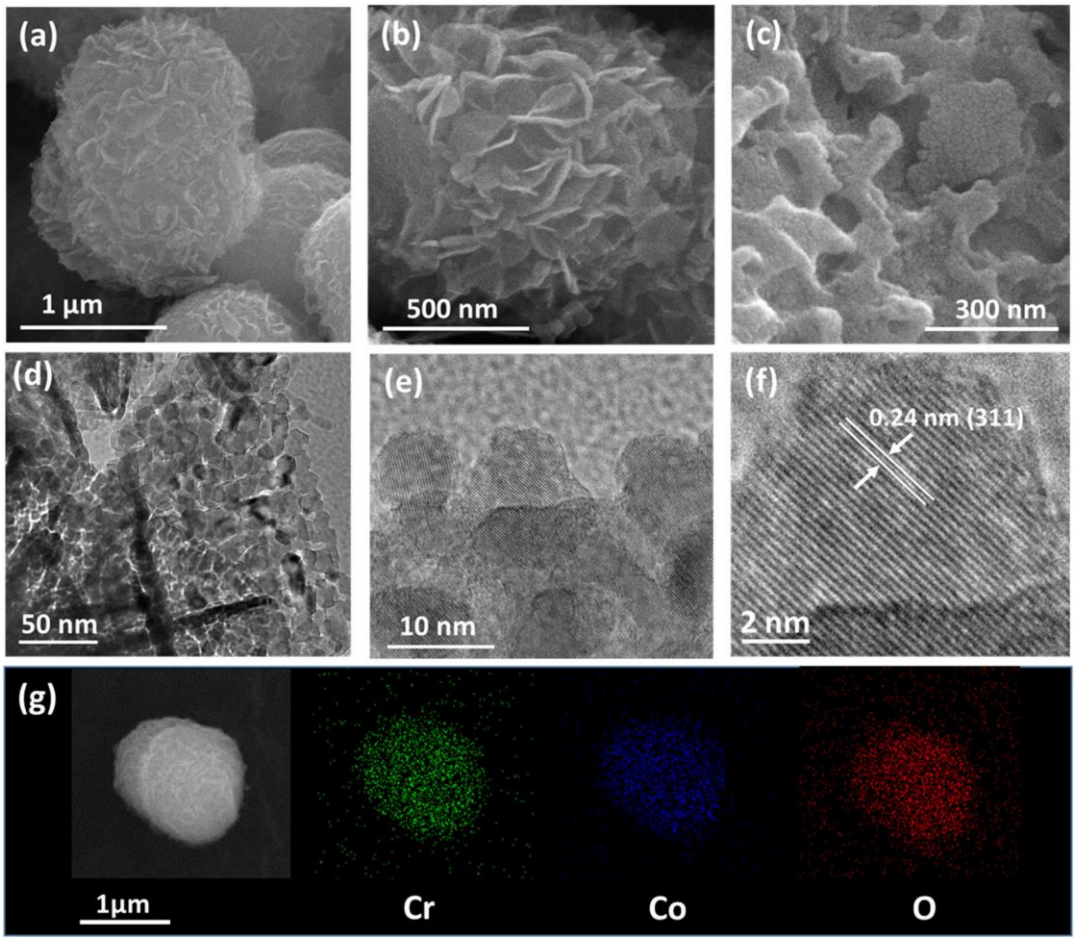

Figure 3.2 a–c SEM and d–f TEM images at different zoom rates, and g element mapping (Co (blue), Cr (green), O (red)) of Co_2CrO_4 microspheres.

Then, the details of the structure of the synthesized microspheres were further investigated by TEM analyses. Due to the TEM images, it can be reported that individual NPs with 12 nm ± 5 nm size assemble to form nanoplates, which is agreeable with the results given by the SEM analysis (Figure 3.2 (d-f)). The high-resolution TEM image provides interlayer spacing of the microspheres which is reported as 0.24 nm corresponding the (311) plane of the Co_2CrO_4. Elemental mapping was used to show the element distribution along the microspheres and the analyses show that there is an even distribution of these elements across the

synthesized material (Figure 3.2 (g)). Also, EDX analysis helps to reveal the basic elemental composition of the hierarchical microspheres and it demonstrates that the synthesized material is composed of Cr, Co and O elements (Figure 3.3).

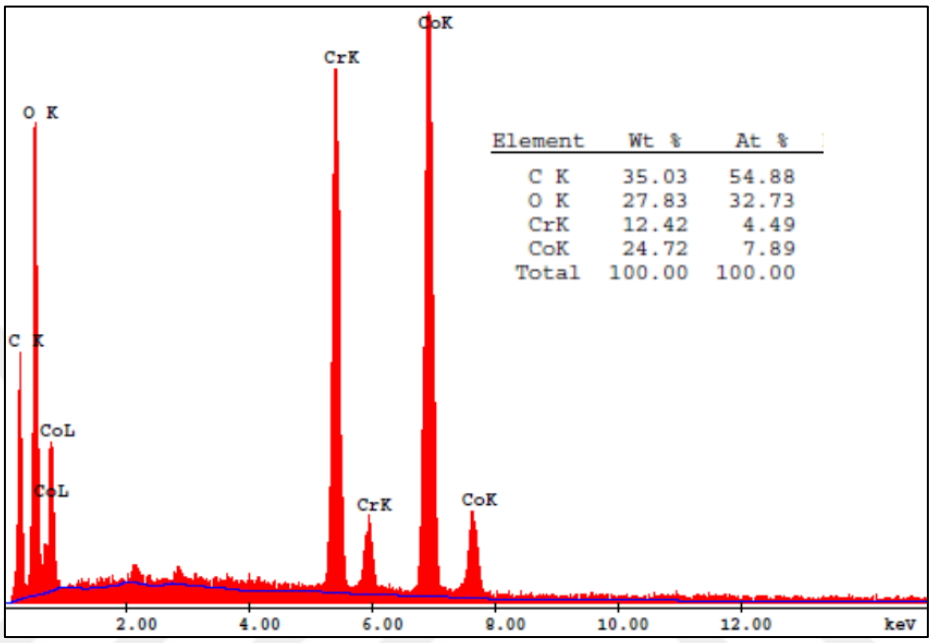

Figure 3.3 EDX spectrum of Co_2CrO_4 microspheres.

The XRD pattern of Co_2CrO_4 microspheres are given in Figure 3.4. At 2θ values, 19.1°, 31.2°, 36.9°, 38.6°, 44.8°, 55.7°, 59.4°, 63.7°, 65.4°, and 77.6° peaks are observed which are the characteristic peaks of spinel Co_2CrO_4 structure and they can be ascribed to (111), (220), (311), (222), (400), (422), (511), (220), (440), and (533) planes of Co_2CrO_4 (PDF card no. 00-024-0326). XRD peak analysis can be used to determine the crystallite size of the synthesized materials and with the help of Debye-Scherrer equation [37], for the diffraction peak at 36.9° the analysis reported the size of Co_2CrO_4 crystallites as ca. 17 nm. This result is comparable to the particle size reported by TEM analysis.

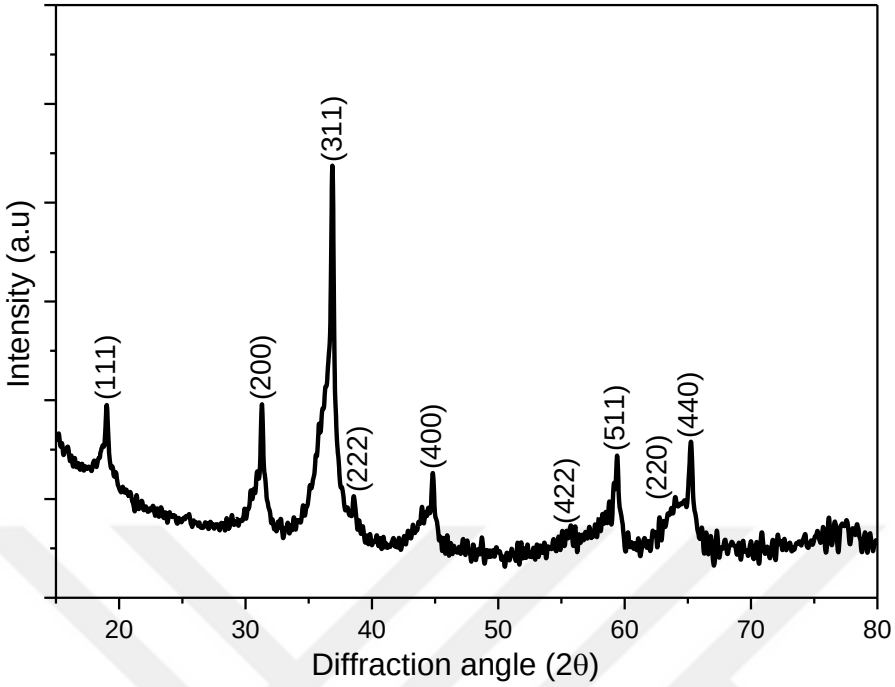

Figure 3.4 XRD pattern of Co_2CrO_4. (JCPDS Card No. 00-024-0326)

In Figure 3.5, the XPS spectra of Co_2CrO_4 microspheres are shown. The survey spectrum demonstrates the existence of Cr, Co, and O elements in the sample along with C, which was used for calibration (Figure 3.5 (a)). In figure 3.5 (b), Cr 2p XPS spectrum demonstrates the two bands of Cr $2p_{1/2}$ and Cr $2p_{3/2}$ at 584.2 eV and 575.1 eV, respectively. Applying Gaussian fit resulted two peaks, which are assigned to Cr^{3+} (583.5 eV and 574.4 eV) and Cr^{6+} (585.2 eV and 576.5 eV) ions [44,45]. It is not common to expect observing Cr^{6+} in AB_2O_4 structure. However, the oxidation of Cr^{3+} ions on the microspheres' surface can lead to the presence of Cr^{6+} ion in the synthesized materials [44]. In figure Figure 3.5 (c), the Co 2p core-level XPS spectrum is demonstrated with the peaks of Co $2p_{1/2}$ (794.1 eV) and Co $2p_{3/2}$ (778.2 eV) peaks as well as their shake-up satellite peaks. Further resolving of the peaks into two Gaussian peaks demonstrates the existence of Co^{3+} (780.5 eV and 795.1 eV) and Co^{2+} (778.2 eV and 793.3 eV), which agree well with previously reported values [46–

[49]. In Figure 3.5 (d), it is shown that the O 1s spectrum produces a band at 528.1 eV with a shoulder at 529.4 eV and the further fitting process yielded three peaks at 527.9 eV, 528.9 eV, 531.7 eV which are assigned to metal-oxygen bonds (I), low oxygen coordination sites (II) and oxygen species (i.e., O_2^{2-}, OH^-) adsorbed onto the catalyst surface (III), respectively [11,50–52].

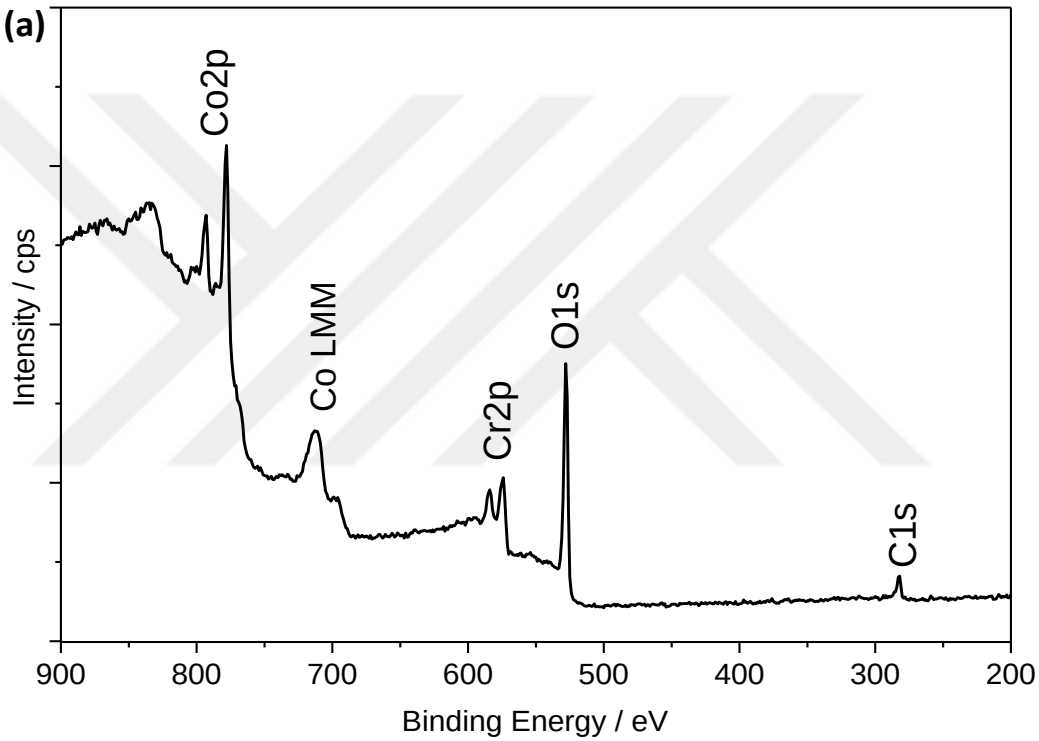

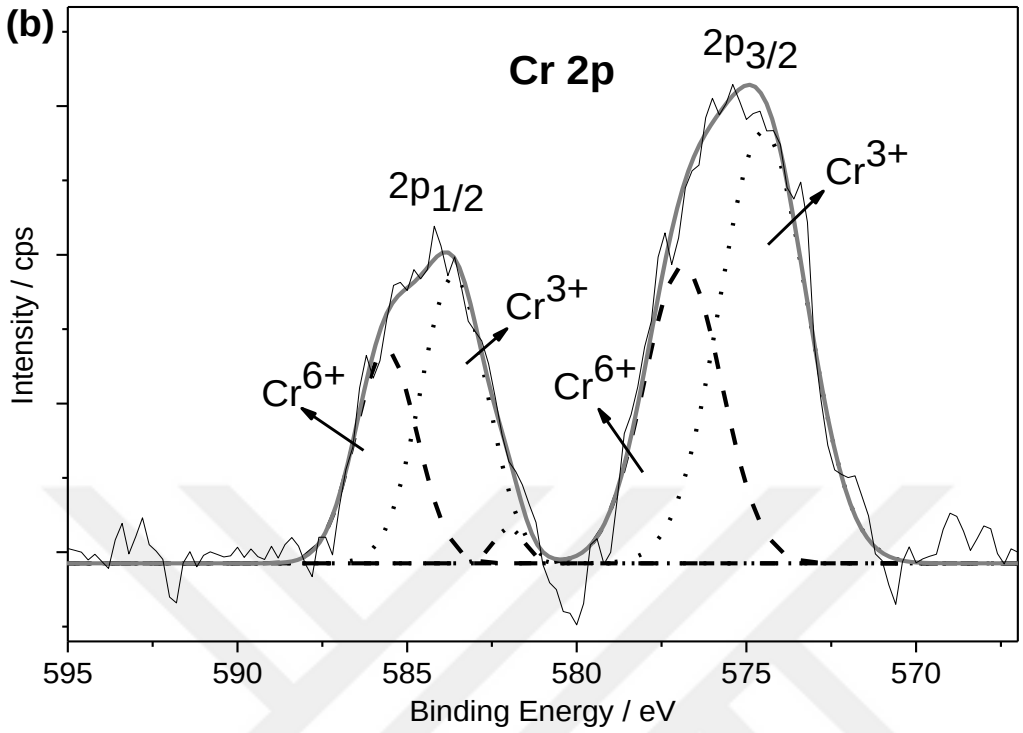
(b)
Cr 2p
2p3/2
2p1/2
Cr3+
Cr3+
Cr6+
Cr6+
Intensity / cps
595
590
585
580
575
570
Binding Energy / eV

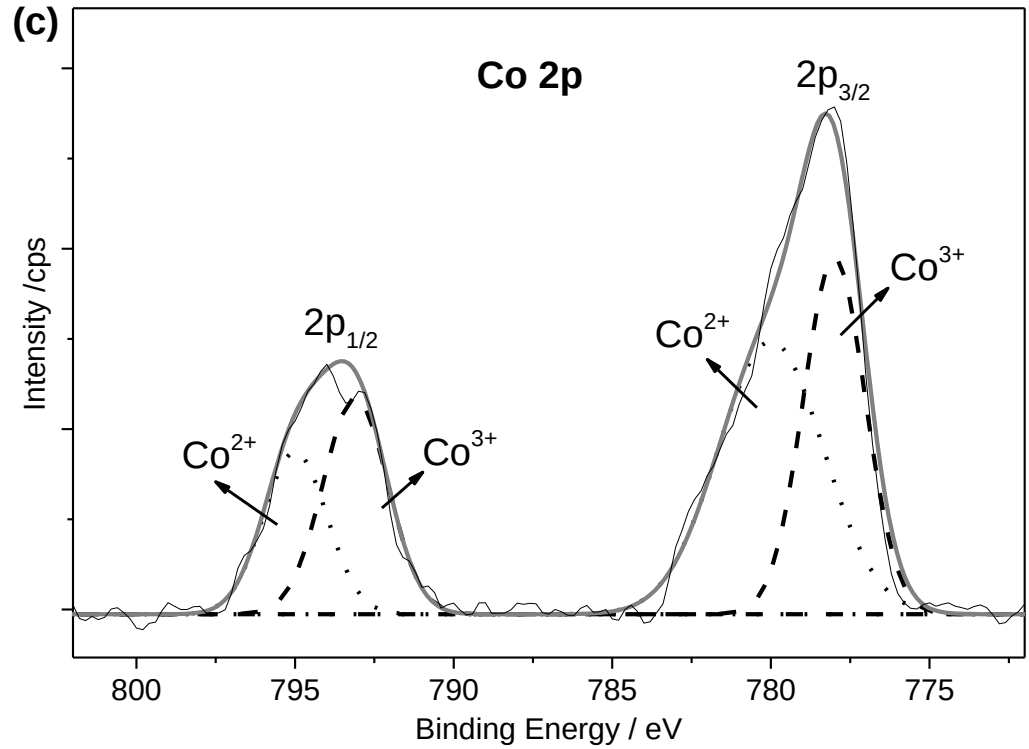
(c)
Co 2p
2p3/2
2p1/2
Co3+
Co2+
Co2+
Co3+
Intensity /cps
800
795
790
785
780
775
Binding Energy / eV

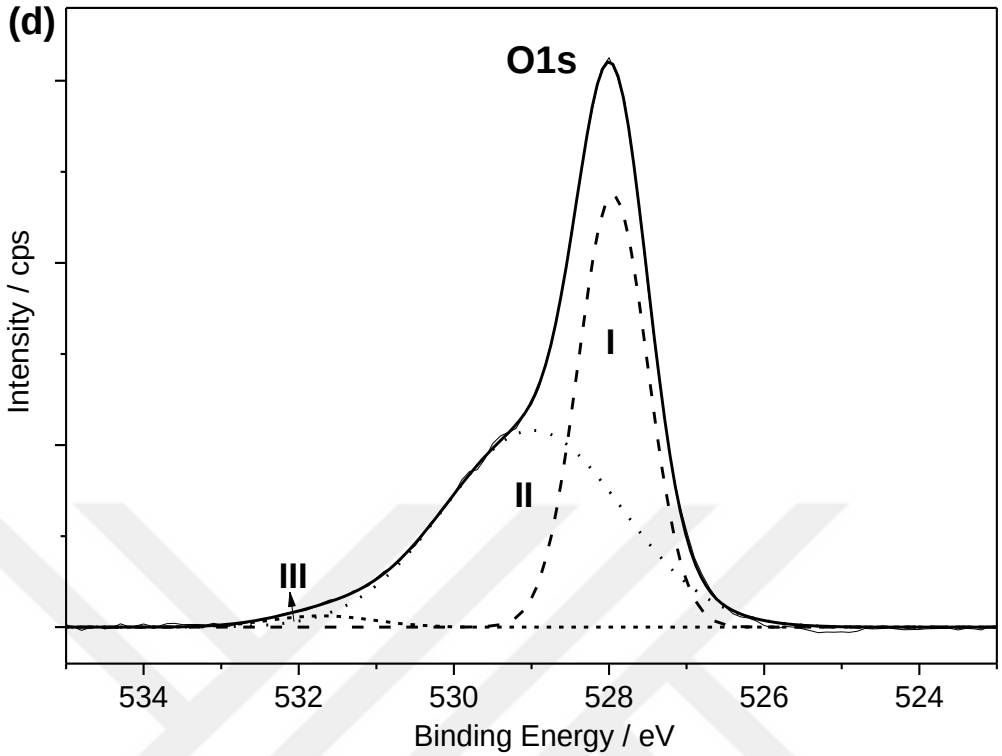

Figure 3.5 XPS of (a) survey spectrum, (b) Cr 2p, (c) Co 2p, (d) O 1s of Co_2CrO_4 microspheres.

To investigate the surface area and the pore size of Co_2CrO_4 microspheres, BET was used. In Figure 3.6, nitrogen adsorption-desorption isotherm is given demonstrating the hysteresis loop at a relative pressure range of 0.4 - 0.6. With the help of the observed isotherm, it can be reported that the Co_2CrO_4 microspheres have a mesoporous nature with a pore size of 3.8 nm. Further researches show that the specific BET surface area measured as 125.3 m^2 g^{-1} and the pore volume of the synthesized microspheres is 0.23 cm^3 g−1. These results imply that our catalyst has high porosity and large surface area which lead to the high interaction of catalyst with reactants as well as reaction intermediates, thus play key role in the catalytic performance of Co_2CrO_4 microspheres.

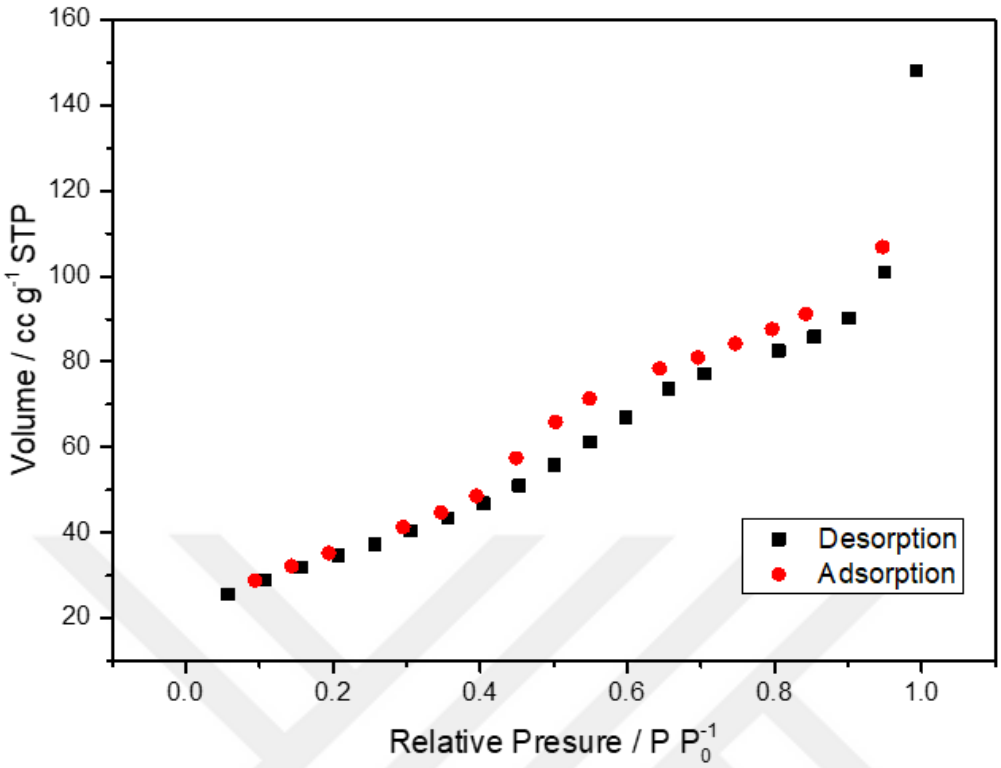

Figure 3.6 N_2 adsorption - desorption isotherm of Co_2CrO_4 microspheres.

3.2 Investigation of Electrocatalytic Activity of Co_2CrO_4 microspheres

With the help of the linear sweep voltammetry, the OER electrocatalytic activity of Co_2CrO_4 microspheres were observed in alkaline medium (0.1 M KOH). For comparison, besides Co_2CrO_4-modified GCE (Co_2CrO_4-GCE), the polarization curves of bare GCE, RuO_2-modified GCE (RuO_2-GCE) and Co_3O_4-modified GCE (Co_3O_4-GCE) were also investigated. In Figure 3.7 (a), it is shown that the onset potential of Co_2CrO_4-GCE is 1.52 V (vs RHE) which proves the significant improvement in the catalytic activity. While this value is comparable with the onset potential of RuO_2 (1.47 V vs RHE), it is also even better than the ones reported previously with the same electrode system modified with similar cobalt-based catalysts such as Co_3O_4 (1.60 V vs RHE), $MnCo_2O_4$ (1.53 V vs RHE), $ZnCo_2O_4$

(1.78 V vs RHE), $NiCo_2O_4$ (1.63 V vs RHE), $CuCo_2O_4$ (1.71 V vs RHE), and $MgCo_2O_4$ NPs (1.63 V vs RHE) [8,13,52,53].

Another way to study the catalytic activity of the OER process with the synthesized catalyst is Tafel analysis. With the Tafel analysis the reaction kinetics can be evaluated by determining the Tafel slope and it is calculated by the fitting process of linear part of the polarization curves. The slopes of the overpotential (η) versus log(j) (j: current density) plots give the Tafel slopes [53]. Figure 3.7 (b) shows the Tafel plots and slopes of Co_2CrO_4-GCE and the Tafel slopes of Co_3O_4-GCE and RuO_2-GCE for comparison. The Tafel slope of Co_2CrO_4-GCE was measured as 106 mV dec^{-1} which is slightly higher than Co_3O_4-GCE and RuO_2-GCE which are 99 mV dec^{-1} and 71 mV dec^{-1}, respectively. In Table 3.1, the Tafel slopes of early reported catalysts are given and it can be seen that the Tafel slope of Co_2CrO_4-GCE has comparable or smaller value than those catalysts (for $MnCo_2O_4$: 101 mV dec^{-1}, for $ZnCo_2O_4$: 135 mV dec^{-1}, for $NiCo_2O_4$: 85 mV dec^{-1}, and for $NiCo_2O_4$ NPs: 139 mV dec^{-1}) [8,52,53].

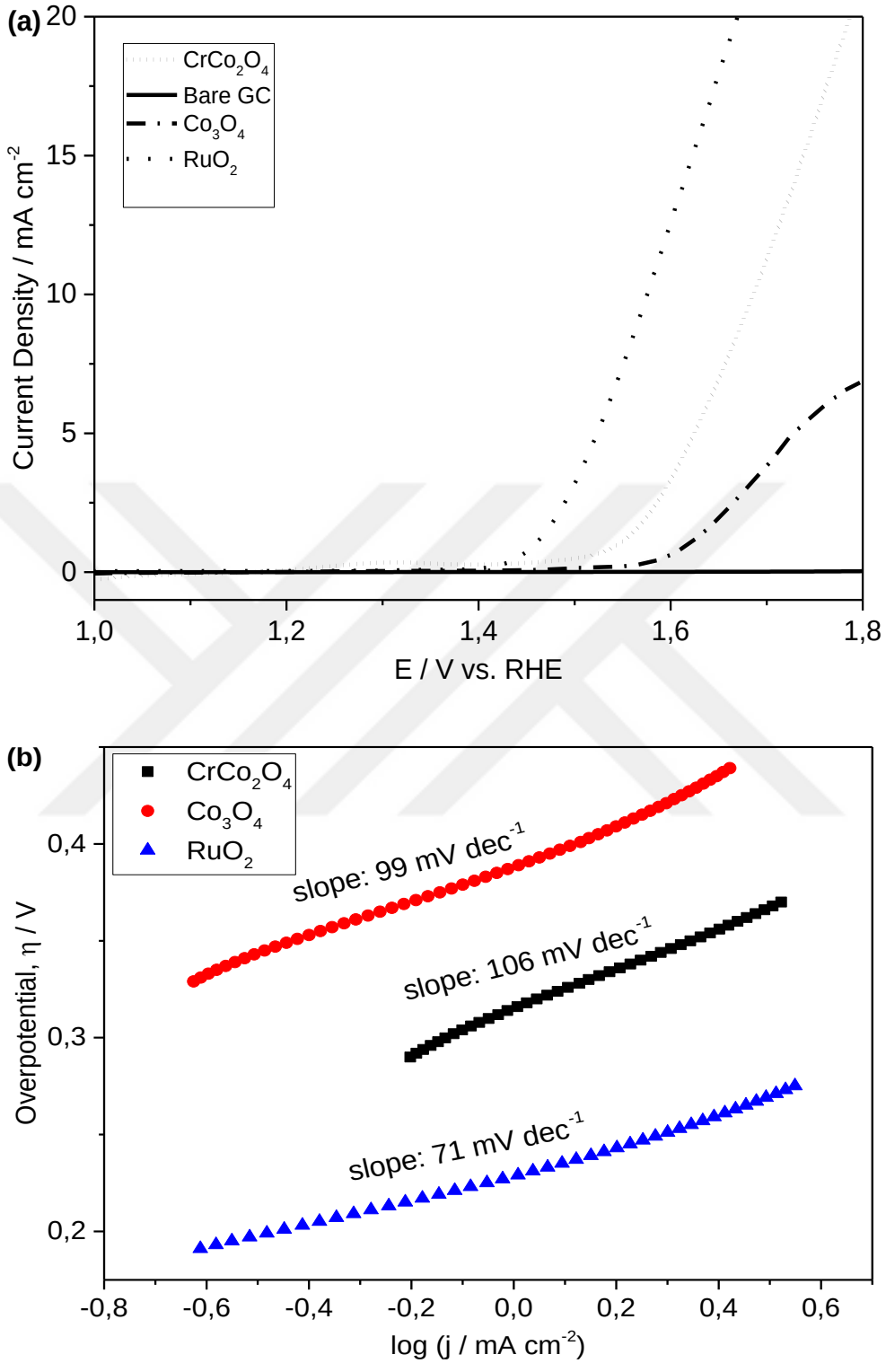

Figure 3.7 a) Polarization curve of Co_2CrO_4, Co_3O_4, and RuO_2 and b) the corresponding Tafel plots.

As mentioned before, the overpotential value at the current density of 10 mA cm^{-2} (η_{10}) is very important while investigating the catalytic performance of the electrocatalyst [3,54–56]. The overpotential value for Co_2CrO_4-GCE is 456 mV to reach the current density of 10 mA cm^{-2}. Even this value is higher than that of RuO_2 (η_{10} = 346 mV), it is comparable to some of the previously reported values of cobalt-based catalysts (i.e., Co_3O_4 (η_{10} = 426 mV), $MnCo_2O_4$ (η_{10}= 411 mV), $MgCo_2O_4$ (η_{10}= 463 mV), $ZnCo_2O_4$ (η_{10} = 570 mV), $NiCo_2O_4$ (η_{10} = 440 mV), and $NiCo_2O_4$ NPs (η_{10} = 430 mV)) [8,13,52,53]. The following table (Table 3.1) compares the results obtained from Co_2CrO_4-GCE and the similar catalysts that are recently reported in the literature.

Table 3.1 Summary of some recently reported representative OER electrocatalysts in alkaline medium together with the data obtained for Co_2CrO_4 nanostructures.

	Onset Potential (vs RHE) (V)	**η_{10} (mV)**	**Tafel slope (mV dec^{-1})**	**Medium**	**REF**
$CrCo_2O_4$	1.52	456	106	0.1 M KOH	This work
Co_3O_4	1.60	-	99	0.1 M KOH	This work
RuO_2	1.47	346	71	0.1 M KOH	This work
$MgCo_2O_4$	1.63	463	75	0.1 M KOH	[13]
$MnCo_2O_4$	1.53	411	101	0.1 M KOH	[8]
$NiCo_2O_4$	1.63	440	85	1.0 M KOH	[53]
$CuCo_2O_4$	1.71	460	101	1.0 M KOH	[53]
$ZnCo_2O_4$	1.78	570	139	1.0 M KOH	[53]

The synthesized catalyst then further investigated for its electrocatalytic activity by electrochemically active surface area (ECSA) and surface roughness factor (RF) since they give information about the number of the active sites on the surface of the catalyst. As mentioned before, the calculation of ECSA can be reached from double-layer capacitance (Cdl) of a catalyst surface (Equation 1.4). To reach Cdl value cyclic

voltammograms (CVs) at non-Faradaic potential range (from 1.077 to 1.177 V vs RHE) were taken at different scan rates (Figure 3.8 (a)). At constant potential of 1.159 V vs RHE, the double-layer charging current versus scan rate graph was plotted and it produced a straight line which gives a slope resulting the Cdl value of the catalyst (Figure 3.8 (b)). After these steps, Cdl and ECSA values of the Co_2CrO_4 microspheres were calculated as 0.064 mF and 1.06 cm^2, respectively. The Cdl and ECSA values were also calculated for Co_3O_4 for comparison and founded as 0.00872 mF and 0.1453 cm^2, respectively. Then, RF value, which is determined by the ratio of ECSA to geometric area of the GC electrode (0.07 cm^2), was calculated and founded as 15.14 for Co_2CrO_4 and 2.076 for Co_3O_4. The mass activity, another important parameter for the electrocatalytic activity, were calculated as 25 A g^{-1} and as 8.13 A g^{-1} for Co_2CrO_4 and Co_3O_4 respectively at an overpotential of 456 mV. Table 3.2 summarizes the comparison of the parameters above for Co_3O_4 and Co_2CrO_4 catalysts. Higher values of these parameters (mass activity, ECSA and RF values) of Co_2CrO_4 catalyst than the values of Co_3O_4 implies that the integration of another metal, chromium, into Co_3O_4 spinel structure results an improvement in electrocatalytic performance and gives encouraging results to make Co_2CrO_4 a new and successful catalyst for OER applications.

Table 3.2 Summary of comparison of double-layer capacity (Cdl), electrochemically active surface area (ECSA), roughness factor (RF) and mass activity of Co_3O_4 and Co_2CrO_4 catalysts.

	Cdl (mF)	**ECSA (cm^2)**	**RF**	**Mass Activity (A g^{-1})**
Co_2CrO_4	0.064	1.06	15.14	25
Co_3O_4	0.00872	0.1453	2.076	8.13

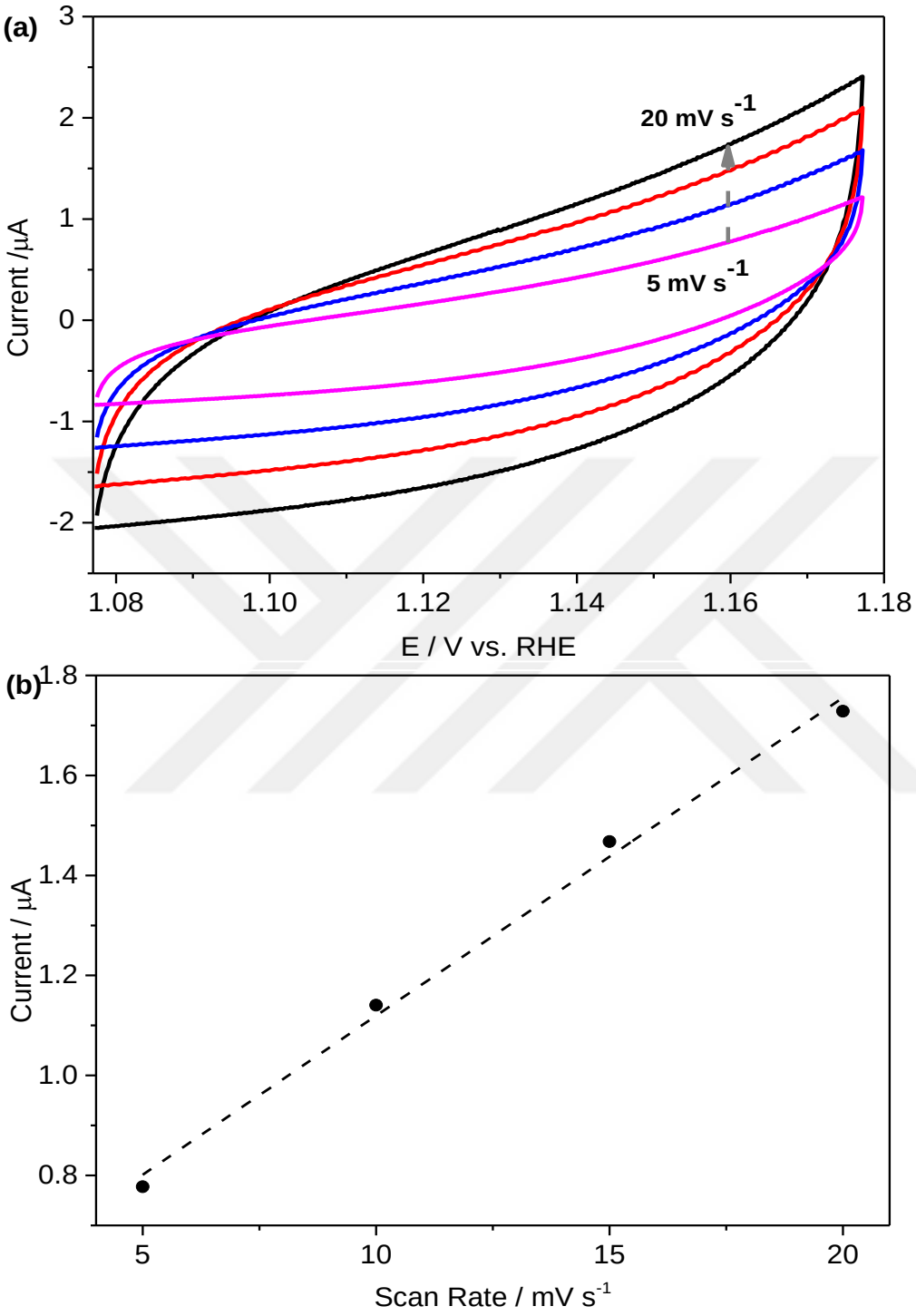

Figure 3.8 (a) Cyclic Voltammetry measured at different scan rates from 5 to 20 mV s−1, (b) plot of current at 1.159 V vs the scan rate of Co_2CrO_4 microspheres.

The most important step to evaluate the electrocatalytic potential of the synthesized catalyst is the stability measurement. Constant potential electrolysis in alkaline solution (0.1 M KOH) was applied to determine the stability of the catalyst. The process was conducted by applying an overpotential of 457 mV (μ_{10}) to Co_2CrO_4-modified GCE for 4 hour and changes in the current density were observed. A decrease in the current density was observed over 4 hours of electrolysis (Figure 3.9). While performing constant potential electrolysis, unprevented oxygen gas bubbles may form during the process which may block the electrode's surface and the usage of the same working electrode in electrolysis process for multiple times may cause more of these blockades.

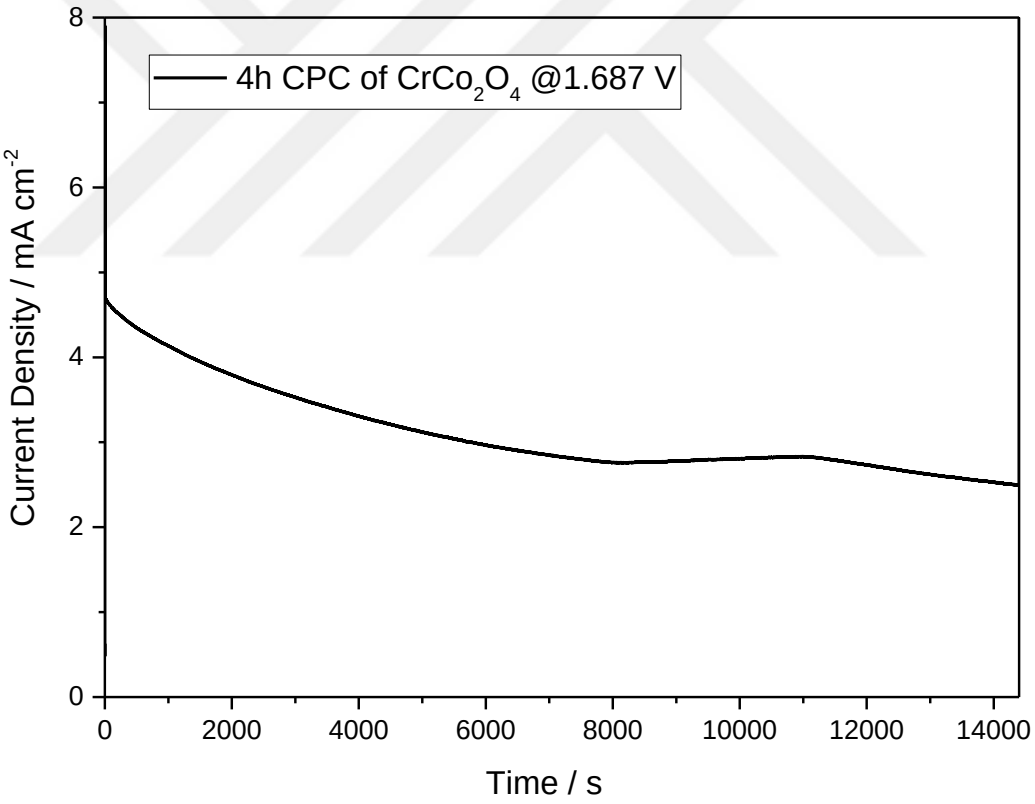

Figure 3.9 The change in current density during chronoamperometric electrolysis of Co_2CrO_4 microspheres at 0.1 M KOH.

To ensure whether this decrease changes the performance of the catalyst the polarization curves were recorded before and after electrolysis and almost no change was observed in onset potential after the constant potential electrolysis. In addition to this result, the overpotential value at current density of 10 mA cm^{-2} also stays unchanged after 4 hours of electrolysis (Figure 3.10). Hence, it can be reported that the Co_2CrO_4 microspheres are stable catalysts under alkaline conditions.

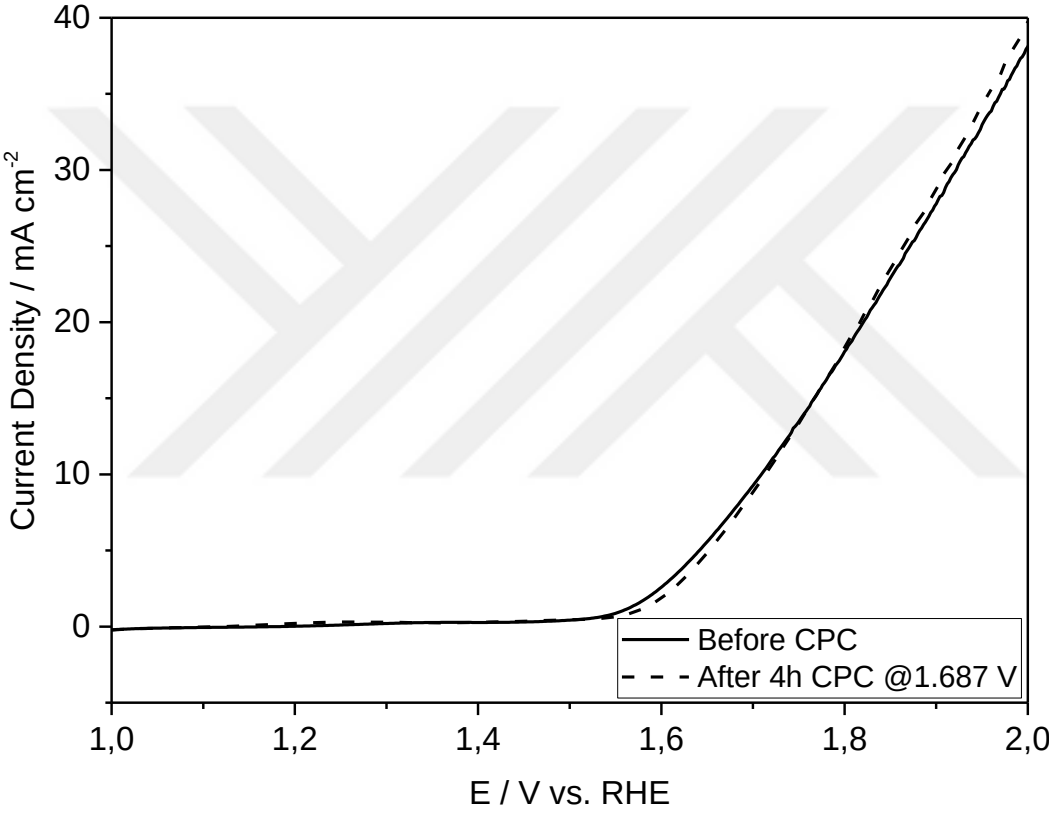

Figure 3.10 Polarization curve of GCE-Co_2CrO_4 electrode recorded before and after the stability test in constant potential electrolysis in 0.1 M KOH at overpotentials corresponding to initial current density of 5 mA cm^{-2}.

CONCLUSION

The aim of this thesis study was synthesis and characterization of a water oxidation electrocatalyst which is composed of earth abundant elements. For this study, transition metal oxides were investigated. Among all of the transition metals, chromium and cobalt elements were chosen due to their synergetic interaction provided by high electronegativity and good electron transfer properties of them.

Chromium and cobalt elements form hierarchical chromium cobalt oxide microspheres in inverse spinel form. After the synthesis, the characterization and electrochemical performans of these Co_2CrO_4 microspheres as electrocatalysts has been investigated for water splitting process using various techniques.

For the synthesis part, CTAB directed hydrothermal method was used. The characterization of Co_2CrO_4 microspheres were done using different analytical techniques such as SEM, TEM, EDX-mapping, XRD, XPS, and BET. SEM and TEM results show that the microspheres have hierarchical structures which are formed from nanoplates of Co_2CrO_4 nanoparticles with 12 ± 5 nm size. BET analysis gives information about their mesoporous structure with 3.8 nm pore size and surface area of 125 $m^2\ g^{-1}$.As the results of all of these analytical techniques, the desired material was well synthesized and provides the characteristics of a good catalyst.

Electrocatalytic performances were also investigated to prove that Co_2CrO_4 microspheres have desired catalytic performance for OER in alkaline medium. This investigation revealed that Co_2CrO_4-CTAB modified GC electrodes had an onset potential of 1.52 V vs RHE and 456 mV overpotential was enough to reach a current density of 10 mV cm^{-2}. In addition to this result, the Co_2CrO_4 microspheres

performed very good stability during constant potential electrolysis for 4 hours with almost no change in onset potential and overpotential even after 4 hours.

These results were reported as an article with co-writers Prof. Dr. Emren NALBANT and Dr. Asude ÇETİN, named as 'Hierarchical Microspheres of Co_2CrO_4 Nanoplatesfor Electrocatalytic Water Oxidation' in Journal of Nanoparticle Research[57].

In the light of these information, it can be concluded that the Co_2CrO_4 microspheres are new and bright addition to the OER electrocatalyst family with their different morphologies, high stabilities, as well as their cost effective and facile synthesis from earth abundant elements.

REFERENCES

1. Zhao, Q., Yan, Z., Chen, C. & Chen, J. Spinels: Controlled Preparation, Oxygen Reduction/Evolution Reaction Application, and Beyond. *Chem. Rev.* **117**, 10121–10211 (2017).

2. Faber, M. S. & Jin, S. Earth-abundant inorganic electrocatalysts and their nanostructures for energy conversion applications. *Energy Environ. Sci.* **7**, 3519–3542 (2014).

3. Suen, N.-T. *et al.* Electrocatalysis for the oxygen evolution reaction: recent development and future perspectives. *Chem. Soc. Rev.* **46**, 337–365 (2017).

4. Li, L., Wang, P., Shao, Q. & Huang, X. Metallic nanostructures with low dimensionality for electrochemical water splitting. *Chem. Soc. Rev.* **49**, 3072–3106 (2020).

5. Lee, Y., Suntivich, J., May, K. J., Perry, E. E. & Shao-Horn, Y. ni z. *J. Phys. Chem. Lett.* **3**, 399–404 (2012).

6. Yang, H. *et al.* Lateral-Size-Mediated Efficient Oxygen Evolution Reaction: Insights into the Atomically Thin Quantum Dot Structure of $NiFe_2O_4$. *ACS Catal.* **7**, 5557–5567 (2017).

7. Fang, Z., Hao, Z., Dong, Q. & Cui, Y. Bimetallic $NiFe_2O_4$ synthesized via confined carburization in NiFe-MOFs for efficient oxygen evolution reaction. *J. Nanoparticle Res.* **20**, 106 (2018).

8. Sun, C. *et al.* Nanowires assembled from $MnCo_2O_4$@C nanoparticles for water splitting and all-solid-state supercapacitor. *Nano Res.* **9**, 1300–1309 (2016).

9. Li, M. *et al.* Facile synthesis of electrospun MFe_2O_4 (M = Co, Ni, Cu, Mn) spinel nanofibers with excellent electrocatalytic properties for oxygen

evolution and hydrogen peroxide reduction. *Nanoscale* **7**, 8920–8930 (2015).

10. Liu, G., Gao, X., Wang, K., He, D. & Li, J. Uniformly mesoporous $NiO/NiFe_2O_4$ biphasic nanorods as efficient oxygen evolving catalyst for water splitting. *Int. J. Hydrogen Energy* **41**, 17976–17986 (2016).

11. Zhao, W. *et al.* Urchin-like $NiO–NiCo_2O_4$ heterostructure microsphere catalysts for enhanced rechargeable non-aqueous $Li–O_2$ batteries. *Nanoscale* **11**, 50–59 (2019).

12. Wei, B. *et al.* $NiCo_2O_4$ nanowire arrays rich in oxygen deficiencies for hydrogen evolution reaction. *Int. J. Hydrogen Energy* **44**, 6612–6617 (2019).

13. Ekebas, E., Cetin, A., Önal, A. M. & Nalbant Esenturk, E. Magnesium substituted cobalt spinel nanostructures for electrocatalytic water oxidation. *J. Appl. Electrochem.* **49**, 315–325 (2019).

14. Cetin, A. & Esenturk, E. N. Hierarchical nanowire and nanoplate-assembled $NiCo_2O_4–NiO$ biphasic microspheres as effective electrocatalysts for oxygen evolution reaction. *Mater. Today Chem.* **14**, 100215 (2019).

15. Ge, J. *et al.* Suppressed Jahn–Teller Distortion in $MnCo_2O_4@Ni_2P$ Heterostructures to Promote the Overall Water Splitting. *Small* **16**, 1–9 (2020).

16. Shan, J. *et al.* Short-Range Ordered Iridium Single Atoms Integrated into Cobalt Oxide Spinel Structure for Highly Efficient Electrocatalytic Water Oxidation. *J. Am. Chem. Soc.* **143**, 5201–5211 (2021).

17. Selvakumar, K., Duraisamy, V. & Senthil Kumar, S. M. Activity manifestationviaarchitectural manipulation by cubic silica-derived Co_3O_4 electrocatalysts towards bifunctional oxygen electrode performance. *New J. Chem.* **45**, 16913–16925 (2021).

18. Hong, J. S. *et al.* Nickel-Doping Effect on Mn_3O_4 Nanoparticles for Electrochemical Water Oxidation under Neutral Condition. *Small Methods* **4**,

1–7 (2020).

19. Maiyalagan, T., Jarvis, K. A., Therese, S., Ferreira, P. J. & Manthiram, A. Spinel-type lithium cobalt oxide as a bifunctional electrocatalyst for the oxygen evolution and oxygen reduction reactions. *Nat. Commun.* **5**, 3949 (2014).

20. Cheng, H., Su, C.-Y., Tan, Z.-Y., Tai, S.-Z. & Liu, Z.-Q. Interacting $ZnCo_2O_4$ and Au nanodots on carbon nanotubes as highly efficient water oxidation electrocatalyst. *J. Power Sources* **357**, 1–10 (2017).

21. Zhu, C. *et al.* Nickel cobalt oxide hollow nanosponges as advanced electrocatalysts for the oxygen evolution reaction. *Chem. Commun.* **51**, 7851–7854 (2015).

22. Gardner, G. *et al.* Structural basis for differing electrocatalytic water oxidation by the cubic, layered and spinel forms of lithium cobalt oxides. *Energy Environ. Sci.* **9**, 184–192 (2016).

23. Khan, S. A., Khan, S. B. & Asiri, A. M. Core–shell cobalt oxide mesoporous silica based efficient electro-catalyst for oxygen evolution. *New J. Chem.* **39**, 5561–5569 (2015).

24. Yazdanbakhsh, M. *et al.* Synthesis, characterization and application of nano-sized Co_2CrO_4 spinel catalyst for selective oxidation of sulfides to sulfoxides. *Mater. Res. Bull.* **47**, 413–418 (2012).

25. Zhao, Q. *et al.* Yolk–shell Co_2CrO_4 nanospheres as highly active catalysts for Li–O 2 batteries: understanding the electrocatalytic mechanism. *J. Mater. Chem. A* **5**, 544–553 (2017).

26. Lin, J.-Y. *et al.* Co_2CrO_4 Nanopowders as an Anode Catalyst for Simultaneous Conversion of Ethane to Ethylene and Power in Proton-Conducting Fuel Cell Reactors. *J. Phys. Chem. C* **122**, 4165–4171 (2018).

27. Ge, J., Wu, J., Ye, B., Fan, L. & Jia, J. Hollow rod-like hybrid $Co_2CrO_4/Co_{1-x}S$

for high-performance asymmetric supercapacitor. *J. Mater. Sci. Mater. Electron.* **30**, 1045–1055 (2019).

28. Kung, H. H. Chapter 2 Bulk and Surface Structure of Transition Metal Oxide. in *Transition Metal Oxides: Surface Chemistry and Catalysis* 6–26 (1989).

29. Ashrit, P. Introduction to Transition Metal Oxides and Thin Films. in *Transition Metal Oxide Thin Film based Chromogenics and Devices* 13–72 (Elsevier, 2017).

30. Zweig, J. E., Kim, D. E. & Newhouse, T. R. Methods Utilizing First-Row Transition Metals in Natural Product Total Synthesis. *Chem. Rev.* **117**, 11680–11752 (2017).

31. Brik, M. G., Suchocki, A. & Kamińska, A. Lattice parameters and stability of the spinel compounds in relation to the ionic radii and electronegativities of constituting chemical elements. *Inorg. Chem.* **53**, 5088–5099 (2014).

32. Deepapriya, S. *et al.* Estimating the ionicity of an inverse spinel ferrite and the cation distribution of La-doped $NiFe_2O_4$ nanocrystals for gas sensing properties. *Appl. Phys. A Mater. Sci. Process.* **125**, 1–13 (2019).

33. Niederberger, M. & Pinna, N. *Metal Oxide Nanoparticles in Organic Solvents*. (Springer London, 2009).

34. *Nanocatalysis Synthesis and Applications*. (John Wiley & Sons, Inc., 2013).

35. Sharma, G. *et al.* Novel development of nanoparticles to bimetallic nanoparticles and their composites: A review. *J. King Saud Univ. - Sci.* **31**, 257–269 (2019).

36. Hench, L. L. & West, J. O. N. K. The Sol-Gel Process. 33–72 (1990).

37. Kim, D.-W., Rhee, K.-Y. & Park, S.-J. Synthesis of activated carbon nanotube/copper oxide composites and their electrochemical performance. *J. Alloys Compd.* **530**, 6–10 (2012).

38. Demir, E., Akbayrak, S., Önal, A. M. & Özkar, S. Nanoceria-Supported Ruthenium (0) Nanoparticles: Highly Active and Stable Catalysts for Hydrogen Evolution from Water. *ACS Appl. Mater. Interfaces* **10**, 6299–6308 (2018).

39. Kuo, C.-H. *et al.* Robust Mesoporous Manganese Oxide Catalysts for Water Oxidation. *ACS Catal.* **5**, 1693–1699 (2015).

40. Dong, Y., He, K., Yin, L. & Zhang, A. A facile route to controlled synthesis of Co_3O_4 nanoparticles and their environmental catalytic properties. *Nanotechnology* **18**, 435602 (2007).

41. Zhao, J., Li, X., Cui, G. & Sun, X. Highly-active oxygen evolution electrocatalyzed by an Fe-doped $NiCr_2O_4$ nanoparticle film. *Chem. Commun.* **54**, 5462–5465 (2018).

42. Gao, M. *et al.* Efficient Water Oxidation Using Nanostructured α-Nickel-Hydroxide as an Electrocatalyst. *J. Am. Chem. Soc.* **136**, 7077–7084 (2014).

43. Anantharaj, S. *et al.* Recent Trends and Perspectives in Electrochemical Water Splitting with an Emphasis on Sulfide, Selenide, and Phosphide Catalysts of Fe, Co, and Ni: A Review. *ACS Catal.* **6**, 8069–8097 (2016).

44. Xu, S. *et al.* Perovskite chromates cathode with resolved and anchored nickel nano-particles for direct high-temperature steam electrolysis. *J. Power Sources* **246**, 346–355 (2014).

45. Yao, W., Duan, T., Li, Y., Yang, L. & Xie, K. Perovskite chromate doped with titanium for direct carbon dioxide electrolysis. *New J. Chem.* **39**, 2956–2965 (2015).

46. Sharma, Y., Sharma, N., Subbarao, G. & Chowdarı, B. Studies on spinel cobaltites, $FeCo_2O_4$ and $MgCo_2O_4$ as anodes for Li-ion batteries. *Solid State Ionics* **179**, 587–597 (2008).

47. Silambarasan, M., Ramesh, P. S., Geetha, D. & Venkatachalam, V. A report

on 1D $MgCo_2O_4$ with enhanced structural, morphological and electrochemical properties. *J. Mater. Sci. Mater. Electron.* **28**, 6880–6888 (2017).

48. Gao, H., Li, Y., Zhao, H., Xiang, J. & Cao, Y. A general fabrication approach on spinel MCo_2O_4 (M = Co, Mn, Fe, Mg and Zn) submicron prisms as advanced positive materials for supercapacitor. *Electrochim. Acta* **262**, 241–251 (2018).

49. Guan, X. Morphology-tuned Synthesis of $MgCo_2O_4$ Arrays on Graphene Coated Nickel Foam for High-Rate Supercapacitor Electrode. *Int. J. Electrochem. Sci.* 2272–2285 (2018).

50. Jiménez, V. M., Fernández, A., Espinós, J. P. & González-Elipe, A. R. The state of the oxygen at the surface of polycrystalline cobalt oxide. *J. Electron Spectros. Relat. Phenomena* **71**, 61–71 (1995).

51. Al-Mamun, M. *et al.* Strongly Coupled $CoCr_2O_4$/Carbon Nanosheets as High Performance Electrocatalysts for Oxygen Evolution Reaction. *Small* **12**, 2866–2871 (2016).

52. Mahala, C. & Basu, M. Nanosheets of $NiCo_2O_4$/NiO as Efficient and Stable Electrocatalyst for Oxygen Evolution Reaction. *ACS Omega* **2**, 7559–7567 (2017).

53. Zhao, Y. *et al.* A study of photocatalytic, chemical, and electrocatalytic water oxidation on ACo_2O_4 (A = Ni, Cu, Zn) samples through doping different metal ions. *J. Catal.* **338**, 30–37 (2016).

54. Indra, A. *et al.* Unification of catalytic water oxidation and oxygen reduction reactions: Amorphous beat crystalline cobalt iron oxides. *J. Am. Chem. Soc.* **136**, 17530–17536 (2014).

55. Song, F. & Hu, X. Ultrathin cobalt-manganese layered double hydroxide is an efficient oxygen evolution catalyst. *J. Am. Chem. Soc.* **136**, 16481–16484 (2014).

56. Su, Y. *et al.* Hydrothermal-assisted defect engineering in spinel Co_3O_4 nanostructures as bifunctional catalysts for oxygen electrode. *J. Alloys Compd.* **799**, 160–168 (2019).

57. Aksoy, I., Cetin, A. & Esenturk, E. N. Hierarchical microspheres of Co_2CrO_4 nanoplates for electrocatalytic water oxidation. *J. Nanoparticle Res.* **22**, (2020).